

GRAPHICAL ABSTRACT















21

Sc
39

Y
57

La

RARE EARTH ELEMENTS

58	59	60	61	62	63	64	65	66	67	68	69	70	71
													
Ce	Pr	Nd	Pm β	Sm	Eu	Gd	Tb	Dy	Ho	Er	Tm γ	Yb	Lu

Chemical Sensors for Rare Earth Metal Ions[†]

[†] In the occasion of the retirement of Prof. Mauro Micheloni

Daniele Paderni, Luca Giorgi,* Vieri Fusi, Mauro Formica, Gianluca Ambrosi, and
Mauro Micheloni*

KEYWORDS: Rare earth elements, Lanthanides, Sensor, Fluorescence, Voltammetry,
Potentiometry

CONTENTS

1. Introduction
2. Ligand to metal energy transfer fluorescent sensors
3. Chemical reaction-induced fluorescent sensors
4. Pure-ligand emission sensors
5. Bio-engineered fluorescent sensors
6. Fluorescent supramolecular systems and nanomaterials
7. Electrochemical sensors
8. Conclusion and outlooks

Acknowledgments

References

ABSTRACT

Rare earth elements (REEs) are a group of fifteen elements ranging from lanthanum ($Z=57$) to lutetium ($Z=71$), also called lanthanides. Two further elements, namely scandium ($Z=21$) and yttrium ($Z=39$), are often referred to as REEs because they have chemical properties similar to lanthanides and are commonly found in the same mineral assemblages. The modern applications of these elements are countless. They constitute critical components of many technological devices and new functional materials, as well as they are extensively used in medical diagnostic applications and for these reasons, REEs are raising new interests of scientists worldwide. The search for chemical sensors suitable for selective sensing of trivalent REE ions represents an important and hard challenge because of their complicated coordination properties due to not well-defined stereo-chemical requirements and an uncertain coordination number, especially in aqueous solution. This review focuses on some of the main works published in the area of fluorescent and electrochemical probes for the detection of REE ions.

1. INTRODUCTION

Rare earth elements (REEs) are a group of seventeen metals Sc, Y, La, Ce, Pr, Nd, Pm, Sm, Eu, Gd, Tb, Dy, Ho, Er, Tm, Yb and Lu having similar chemical and physical properties. Fifteen of them, ranging from lanthanum ($Z=57$) to lutetium ($Z=71$), are also called lanthanides, the other two, namely scandium ($Z=21$) and yttrium ($Z=39$), are referred to as REEs due to their chemical properties similar to lanthanides and they are commonly found in the same mineral assemblages [1]. All the REEs are present in the earth soil as salt minerals, most commonly as fluorocarbonates or phosphates but also as fluorite minerals [2,3]; among REEs, promethium, which becomes from the fission

product of ^{238}U , can be found as trace level in uranium minerals as the instable nuclide ^{147}Pm with a half-life of 2.62 years [4,5]. REEs have a strong affinity towards oxygen and are stable mainly as trivalent cations. At a geological level REEs compounds are more present in igneous rocks and argillaceous sediments and particularly in alkaline soils, where the abundance of REEs is higher than in acid ones probably due to the easy removal of soluble hydroxide complexes [6,7]. In addition, lanthanides stick differently to the soil depending on the soil types as reported by the soil solid/liquid partition coefficient (K_d) [6].

In river waters REEs are present at low levels; the highest concentration is $0.3 \mu\text{g}\cdot\text{dm}^{-3}$ for Ce and the lowest $0.002 \mu\text{g}\cdot\text{dm}^{-3}$ for Lu [8]. Despite REEs are relatively abundant in the earth crust, they are not frequently found in concentrated form; for such reason the separation processes of these elements or their compounds as pure substances represent an economically challenging and intriguing task. The isolation of the individual REEs in their metallic form requires complex and expensive metallurgical processes preventing commodity-level production, as a result these metals are considered rare. Table 1 lists the abundance in the earth's crust of REEs and other metals, as reported by Wedephol in 1995 [9], whereas Figure 1 reports a histogram which compares the relative amounts of REEs. Examining the abundance of REEs compared to that of other common metal elements it is evident that lanthanides as well as scandium and yttrium are not rare at all, with the exception of the artificial radioactive element promethium.

Table 1. Abundance of metals in the Earth's crust

Elements	Symbol	Atomic	Crustal

		number	Abundance (ppm)
Nickel	Ni	28	90
Zinc	Zn	30	79
Copper	Cu	29	60
Cerium	Ce	58	60.0
Lanthanum	La	57	30.0
Cobalt	Co	27	30
Neodymium	Nd	60	27.0
Yttrium	Y	39	24.0
Scandium	Sc	21	16.0
Lead	Pb	82	10
Praseodymium	Pr	59	6.7
Thorium	Th	90	6
Samarium	Sm	62	5.3
Gadolinium	Gd	64	4.0
Dysprosium	Dy	66	3.8
Tin	Sn	50	2.2
Erbium	Er	68	2.1
Ytterbium	Yb	70	2.0
Europium	Eu	63	1.3
Holmium	Ho	67	0.8
Terbium	Tb	65	0.7
Lutetium	Lu	71	0.4
Thullium	Tm	69	0.3
Silver	Ag	47	0.08
Gold	Au	79	0.0031
Promethium	Pm	61	10⁻¹⁸

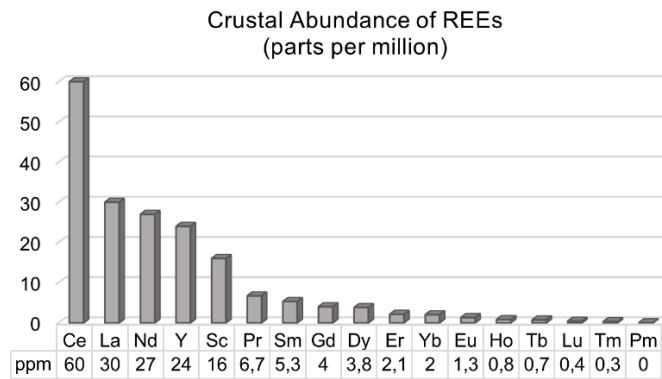


Figure 1. Comparison of the crustal abundance of REEs

On the basis of the trend in crustal abundance and of the geological models relative to the formation of REEs-enriched minerals, these elements have been divided into light (LREEs) and heavy (HREEs) rare earth elements. Figure 2 shows an example of classification reported by Schuler in 2011 [10], but some variations are admitted. For example, some authors classify gadolinium and dysprosium as medium-weight lanthanides.

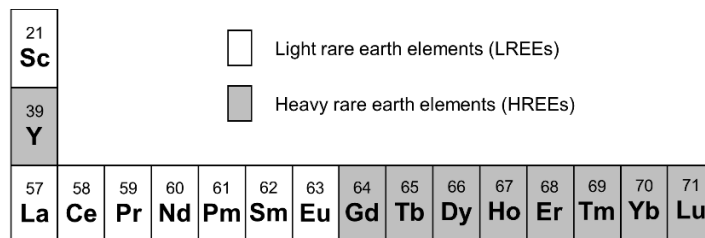


Figure 2. The division between LREEs and HREEs reported by Schuler [10]

The modern applications of REEs are countless, these elements comprise critical components of many technological devices and everyday electronics [11]. Few examples include: yttrium in ceramics, metal alloys, lasers, computer monitors (etc.); lanthanum in electric car batteries, digital cameras (etc.); cerium in catalysts, optical glasses (etc.); neodymium in high-power magnets for laptops, lasers, communication devices (etc.); samarium in high-temperature magnets, electric motors etc.; europium in liquid crystal displays (LCDs), fluorescent lighting systems, glass additives (etc.); gadolinium in NMR imaging contrast agents; terbium in phosphors for lighting and displays; dysprosium and holmium in high power magnets and lasers; ytterbium in fiber-optic technology, solar panels, alloys (etc.); lutetium in X-ray phosphors. In this light, a sharp increase of the global demand for REEs together with the necessity of their recovery and reuse are to be expected thus raising the interest of scientists working in different fields.

In their elementary form REEs are ductile and malleable soft metals, particularly reactive mainly in the form of fine powder as well as at elevated temperature. In aqueous solution REEs are stable above all in their trivalent state, however cerium can be also found as a tetra-positive cation while europium, samarium and ytterbium can be found as divalent ions. The chemical properties of REEs are very similar to each other, and only little variations can be observed along the lanthanide series attributable to the different atomic number and ionic radius, which are inversely correlated. For this reason the REEs chemistry is in continuous development and in particular, the study of the complexation equilibria of REE ions represents an emerging and important field of modern inorganic chemistry [12]. In this context the search of ligands suitable for selective complexation of trivalent REEs metal ions represents a challenging task, considering that the coordination properties of these ions are complicated by not well defined stereo-chemical

requirements and uncertain coordination numbers, especially in aqueous solution. The most stable complexes have been obtained with O-chelating ligands containing $-\text{OH}$, $-\text{O}-$, $=\text{O}$, $-\text{O}^-$ or $-\text{COO}^-$ binding groups as oxalate, citrate, tartrate or β -diketonates; the complexes are characterized by high coordination numbers such as 7, 8, 9 or 12 [13].

The coordination number exhibited by the metal ion belonging to the series can be related to the cationic radius; in particular, using the 18-crown-6 ether as common ligand it has been possible to investigate the species formed and the related coordination number exhibited by the REE ions using the same macrocyclic cavity size.

Several techniques including elemental analysis, FT-IR, NMR, TGA and X-Ray diffraction studies, allowed to observe that the largest lanthanides, from La(III) to Nd(III), form very stable complexes with 1:1 stoichiometry; Sm(III), Eu(III) and Gd(III) form, instead, more stable complexes having 4:3 metal to ligand ratio. Finally, the smallest ions (Tb(III)-Lu(III)) form less stable complexes because their ionic radius is too small to fit the binding cavity of the 18-crown-6 ligand [14,15].

Coordination compounds showing N as binding donor atoms are in smaller number with respect to those showing O-donors, probably because the latter are more often negatively charged, giving rise to a higher stabilization of REE ions due to the essential ionic bonds formation.

The binding of REE with N-donor ligands generally results more efficient in solvents with lower polarity. Alcoholic and polar solvents such as acetonitrile lower the competition of the solvent vs the nitrogen ligand in binding REEs with respect to water molecules thus, typical polyamine ligands such as ethylenediamine, diethylenetriamine, bipyridine and terpyridine are able to form REE complexes in which they show characteristic coordination numbers of 8, 9 or 10. N-O-mixed donor highly-dentate

ligands such as EDTA, DTPA, DOTA, oxa-aza-macrocycles and others form stable complexes also in aqueous solution[16]. Pre-organization of the ligand is an important requirement to stabilize REE metal complexes. Some examples of trivalent lanthanide ion complexes with ligands pre-organized by transition bivalent metal ions, stable also in aqueous solution, have been reported [17-19].

There are many applications for selective ligands able to coordinate REE ions ranging from separation to purification, transport and sensing. In particular, chemosensors are widely used in inorganic, biological, environmental and manufacturing fields for the monitoring of metal ions. In general, a chemosensor is designed to interact with a specific species (neutral molecule, ion, biological macromolecule) and to yield a measurable signal as a response. To obtain a good detection system, some fundamental criteria must be considered during the design, the first being the selective response to the target. Another point to be considered is the response time. The system has to be fast enough in the recognition to allow a practical use of the sensor in its possible applications. For host-guest sensors, this parameter is influenced by the kinetics of the host-guest complex formation, which must be high to allow a rapid detection of the analyte. Even the sensibility of the sensor is an important criterion. A low detection limit means that the species of interest can be detected even in those samples where the concentration of the species of interest is low. The interaction between the sensor and the analyte must involve the change of a physico-chemical parameter, such as the optical or electrochemical properties (Figure 3).

The characterization of the interaction in terms of structural, thermodynamic and kinetic parameters are often crucial to understand such photo-chemical or electro-chemical signals. In this light, several techniques can help to achieve this information; for example,

the time resolved laser fluorescence spectroscopy (TRLFS) is useful to investigate the above parameters and the coordination environment of the trivalent f block elements resolving, for instance, how many water molecules bind Eu or Cm ions in both normal and heavy water solutions [20,21].

Considering the need for a fast and easy obtainable response to the presence of REEs in a sample, great preference is given to fluorescent and electrochemical chemosensors that preserve high efficiency and sensitivity.

For this reason, this review focuses on some important works published in the area of fluorescent and electrochemical organic probes for the detection of rare earth metal ions in solution.

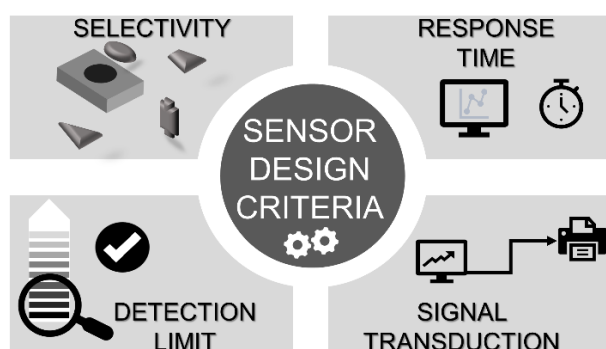


Figure 3. Essential characteristics of a chemosensor

2. LIGAND TO METAL ENERGY TRANSFER FLUORESCENT SENSORS

The spectral properties of lanthanide ions are characterized by the presence of 4f electrons, making them significantly different from the transition metal ions owning nd electrons. The only exceptions are the closed shell f^0 La(III) and f^{14} Lu(III) ions.

The filling of the seven 4f orbitals in lanthanides gives rise to a lot of energetic states allowing a wide possibility of f-f transitions (Figure 4). Moreover, in metal ion complexes, the filled $5p^6 6s^2$ orbitals, shielding the 4f open levels, prevent any interaction of the f orbitals with the ligands. For this reason, most lanthanide ions show a characteristic line-emission of optically pure colors attributed to the f-f transitions that are rather unaffected by the ligand field stabilization.

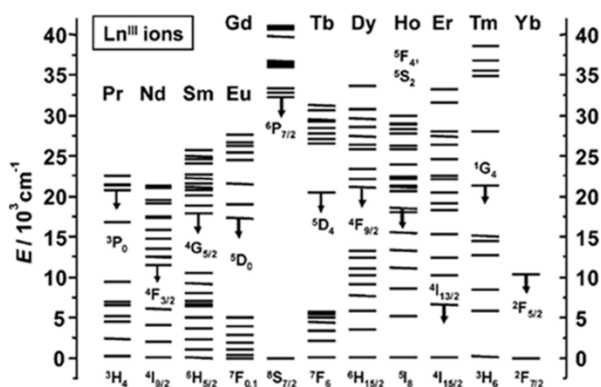


Figure 4. Partial energy diagrams of lanthanide trivalent ions (except La(III), Ce(III), Pm(III), and Lu(III)) showing the ground state and one of the most luminescent excited states (for a given ion, several excited states are usually luminescent, except for Gd(III) and Yb(III)). Reprinted with permission from Ref. [12]. Copyright © 2006, American Chemical Society

Despite their optically pure and easily recognizable emission, these metal ions show scarce absorptivity reflecting in a low ϵ coefficient ($1\text{--}10 \text{ dm}^3 \cdot \text{mol}^{-1} \cdot \text{cm}^{-1}$); the reason is ascribed to the presence of forbidden f-f- transitions mainly caused by spin- and parity-not allowed transitions; thus, the direct excitation of lanthanides by light is not of great

yield [12]. One of the main strategies useful to overcome the scarce REE's photoexcitation is the use of ligands bearing a chromophore. The latter exhibits high efficiency in absorbing light of selected wavelengths giving high absorption coefficients ϵ (10^4 to 10^5 $\text{dm}^3\cdot\text{mol}^{-1}\cdot\text{cm}^{-1}$). The formation of the lanthanide complex allows the transfer of the absorbed energy from the lower excited state of the ligand to an accessible excited state of the coordinated metal ion. This phenomenon is known as "antenna-effect" and allows the enhancement of the emission efficiency of the lanthanide. The overall process comprises the absorption of high energy light radiation by the chromophore, usually followed by a non-radiative energy transfer involving the ligand's excited triplet state T_1 and lanthanide's excited state then, the emission of light from the latter, usually in the visible range, produces the energy decay to the ground state (Figure 5). The design of polydentate ligands able to form stable lanthanide complexes with efficient photochemical properties in terms of ligand-to-metal energy transfer represents an important challenge in advanced photochemistry. The main application of this concept lies on the synthesis of photoactive materials and surfaces, a field extensively studied and explored in the last 20 years [13], but only few examples have been employed in the REEs sensing field. Examining the scientific literature over the last 20 years, very few lanthanide complexes able to emit visible and NIR (near infrared) wavelengths after excitation with visible or UV light are reported. In fact, it is a hard task to obtain emission of Ln(III) complexes in solvents having high-energy vibrational modes, such as water, due to the quenching upon coordination of solvent molecules to the metal center. Thus, suitable ligands for REEs fluorescent sensing need to be highly polydentate in order to completely saturate the coordination requirement of the metal ion. The distance between the organic fluorophore and the metal ion also plays a crucial role; therefore, it is a

promising strategy to incorporate in the molecular framework a fluorophore able to perform the “antenna-effect”.

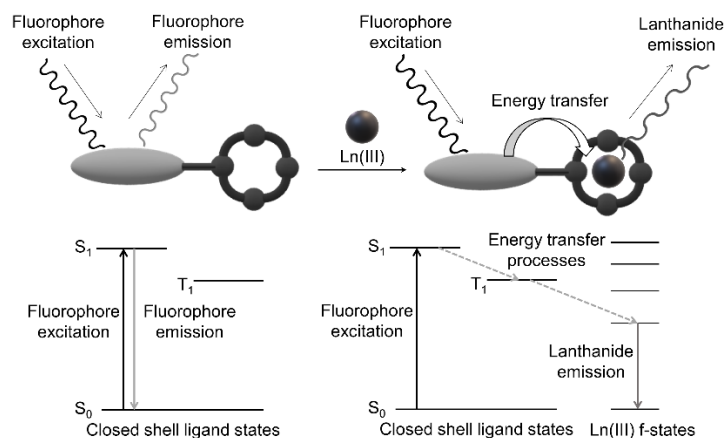


Figure 5. Scheme of the "antenna-effect" and simplified Jablonsky diagram

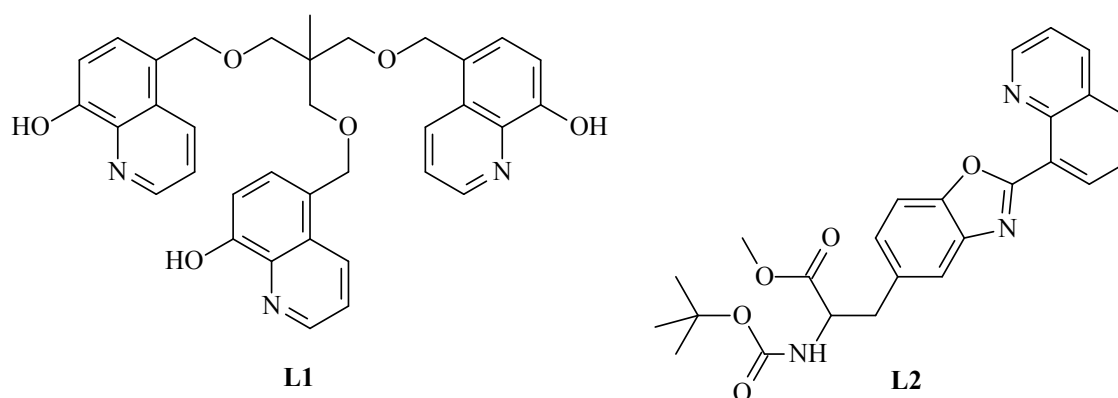
In this chapter we report the most important examples of molecular chemosensors for REE ions in which the signal transduction is due to an energy transfer process from the fluorophore to the lanthanide cation.

The 8-hydroxyquinoline (8-HQ) and related derivatives are suitable metal ion coordinating fragments to be largely used in coordination chemistry both alone as well as taking part of more complex molecular systems. These fragments, in their deprotonated form, are able to coordinate Ln(III) and some complexes have been investigated as suitable materials for the obtainment of electroluminescent devices. Kanungo et al. synthesized the 5-[3[(8-hydroxy-5-quinolyl)methoxy]-2-[8-hydroxy-5-quinolyl]-2-methylpropoxy]quinolin-8-ol ligand (**L1**) (Scheme 1), that behaves as hexadentate tripodal ligand towards metal ions thus being able to coordinate Eu(III), Tb(III), La(III) and Er(III) ions in aqueous media [22,23]. Each hydroxyquinoline moiety shows two acid-base sites, the heterocyclic nitrogen atom and the phenolic OH group. Thus, **L1** can

exist as seven differently protonated species ranging from the anionic H_3L1^{3-} to the cationic H_3L1^{3+} one; the potentiometric experiments showed that this ligand forms mononuclear complexes with Eu(III), Tb(III), La(III) and Er(III) ions with various protonation degrees depending on the pH. In aqueous media the formation constants of the neutral $[LnH_3L1]$ complexes were found to be similar and very high, being $\log\beta = 35.24, 35.23, 36.42$ and 35.76 for Eu(III), Tb(III), La(III) and Er(III), respectively (Table 2). As a consequence, the spectrophotometric and spectrofluorimetric behavior of the complexes resulted complicated, but well described and discussed by the Authors. All the four complexes are fluorescent with intensity and emission wavelength depending on the pH. The main result of the study is that all complexes emitted a strong green fluorescence in the neutral pH-range, with λ_{em} ranging from 510 to 530 nm (λ_{ex} between 330 and 390 nm) depending on the metal ion. This allows to obtain the sensing of the four above mentioned REE ions at physiological pH in the visible range. This system is highly efficient but lacks selectivity, as the $\log\beta$ values highlight, confirming that the selectivity over REE ions is a hard task to be achieved.

Wiczak *et al.* synthesized a quinolinylbenzoxazole-based system, namely N-Boc-3-[2-(8-quinolinyl)benzoxazol-5-yl]alanine methyl ester (**L2**) (Scheme 1), as a potential chemosensor for Zn(II) and rare earth Eu(III) and Tb(III) ions working in acetonitrile solution [24]. Transition metal ions cause substantial changes of absorption and fluorescence spectra; the free ligand absorbs at $\lambda_{max} = 310$ nm and the addition of Zn(II) determines the appearance of two new absorption bands at $\lambda_{max} = 270$ and 350 nm. With regard to the fluorescence emission, the paramagnetic open shell Co(II), Ni(II) and Cu(II) metal ions act as quenchers, while the d^{10} Zn(II) and Cd(II) metal ions cause an increase of the fluorescent signal. However, the latter two enhance the emission quantum yield

without significantly displacing the emission wavelength maximum ($\lambda_{em} \approx 425$ nm). Noteworthy, luminescent rare earth ions such as Eu(III) and Tb(III) cause the appearance of an absorption band at $\lambda_{max} = 370$ nm and the displacement of the emission band from $\lambda_{em} = 425$ to 530 nm. This great red shift is due to the antenna effect, thus this ligand can be used as a chemosensor suitable to detect both Zn(II) and Cd(II) ions, by monitoring the fluorescence at $\lambda_{em} = 425$ nm, as well as REE ions, by monitoring the emission at $\lambda_{em} = 525$ nm.

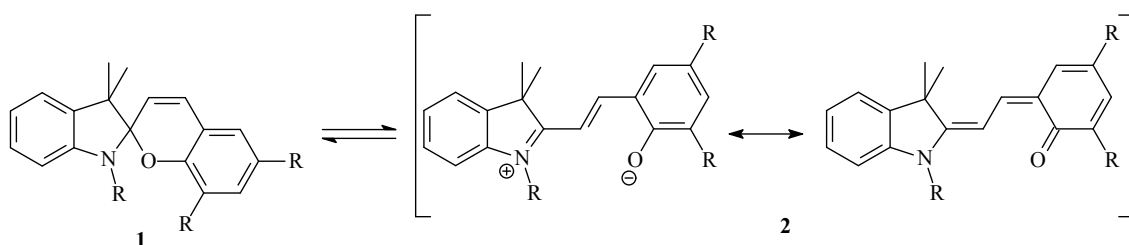


Scheme 1. Structures of **L1** and **L2**

3. CHEMICAL REACTION-INDUCED FLUORESCENT SENSORS

Another important strategy for fluorescence signal transduction is represented by ligands able to coordinate metal ions inducing a chemical reaction. These molecules contain a specific framework that, due to the coordination with a suitable metal ion, undergoes a chemical transformation which drastically changes the photochemical properties of the system. In this chapter, the main examples of reaction-mediated sensors are reported.

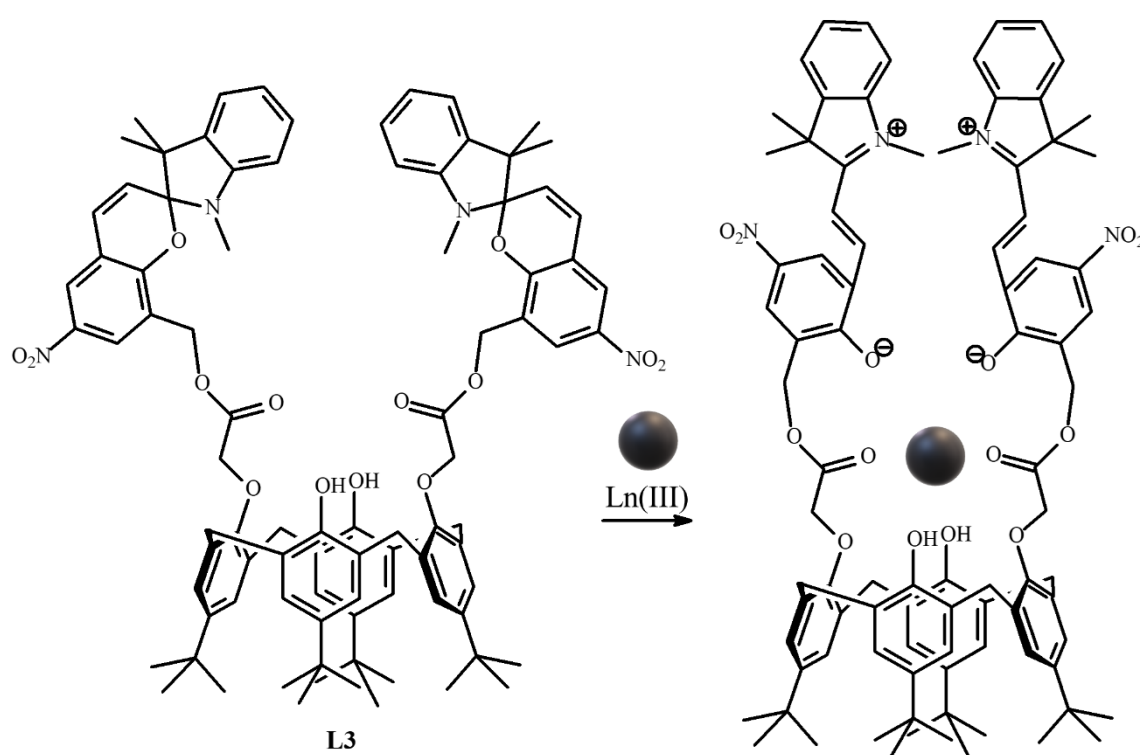
Most of the sensors based on induced chemical reactions contain spirobenzopyran derivatives as the photoactive unit, due to their capability to give a reversible ring-opening reaction upon either UV-irradiation (photochromism) or interaction with hard metal cations [25]. As reported by K. Kruttwig *et al.*, under appropriate conditions the colorless neutral spirolactam form (1) is isomerized to the colored open merocyanine form (2) (Scheme 2), that could be present in the zwitterionic arrangement becoming able to coordinate hard metal ions. The variation of optical properties is caused by the extension of the conjugate π system to the whole molecule occurring upon the ring opening. Louie *et al.*, for example, used a gadolinium(III) complex of a spirobenzopyran-derivatized cyclen-1,4,7-triacetic acid (DO3A) as MRI contrast agent responsive to commonly employed luminescent biomarker systems [26]. Nevertheless, only few examples of the exploitation of this paradigm for chemosensing of REE ions are present in the scientific literature.



Scheme 2. Structure of the neutral spirolactam form (1) and of the isomerized colored open merocyanine form (2)

Gao *et al.* synthesized a receptor based on a calix[4]arene bearing two spirobenzopyran derivatives as side arms, namely 5,11,17,23-tetratert-butyl-25,27-bis[[1',3',3'-trimethyl-6-nitrospiro(2-H-1-benzopyran-2,2'-indoline)-8-yl]methoxyformylmethoxy]-26,28-dihydroxycalix[4]arene (L3) (Scheme 3), able to selectively recognize some REEs over

alkaline, alkaline-earth and transition metal ions in acetonitrile medium [27]. The addition of lanthanide ions to an acetonitrile solution of **L3** causes an immediate change of the solution color from purple to yellow, visible to the naked eye, due to the opening of the spirobenzopyran function. The Authors hypothesized that the driving force for the ring opening is the stronger affinity of lanthanide ions for the zwitterionic form of merocyanine, mediated by electrostatic interaction, than for the neutral spirobenzopyran.

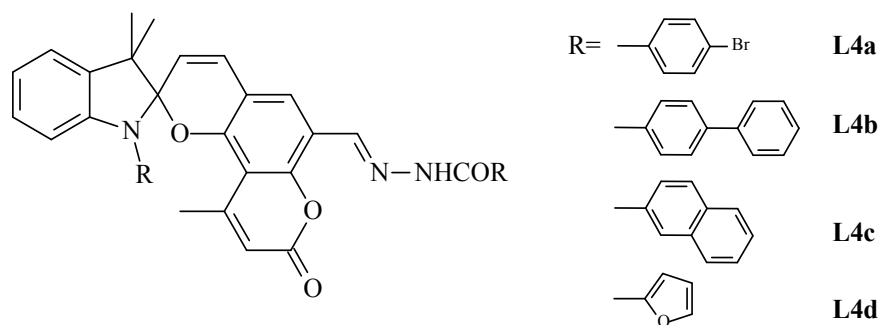


Scheme 3. Structure of **L3** and the proposed coordination sites for Ln(III)

The coordination of metal ions takes place to the lower rim of the receptor in which are present almost eight oxygen atoms which can coordinate to the hard lanthanide ions satisfying the request for a high coordination number. The ability to open the spirobenzopyran ring follows the $\text{Yb(III)} > \text{Er(III)} > \text{Gd(III)} > \text{Dy(III)} > \text{Eu(III)} > \text{Pr(III)} > \text{La(III)}$ trend that is opposite to that of

the lanthanide ionic radii; this suggests that the size fit effect is at the basis of the recognition process. Only the coordination of Eu(III) has been studied through a fluorescence response. **L3** is characterized by a weak red fluorescence band at $\lambda_{em} = 637$ nm ($\lambda_{ex} = 475$ nm), attributed to the $\pi-\pi^*$ transition of the merocyanine open form. The addition of Eu(III) causes a 10-times increase of the emission intensity and its shift toward higher energies (λ_{em} from 637 to 595 nm).

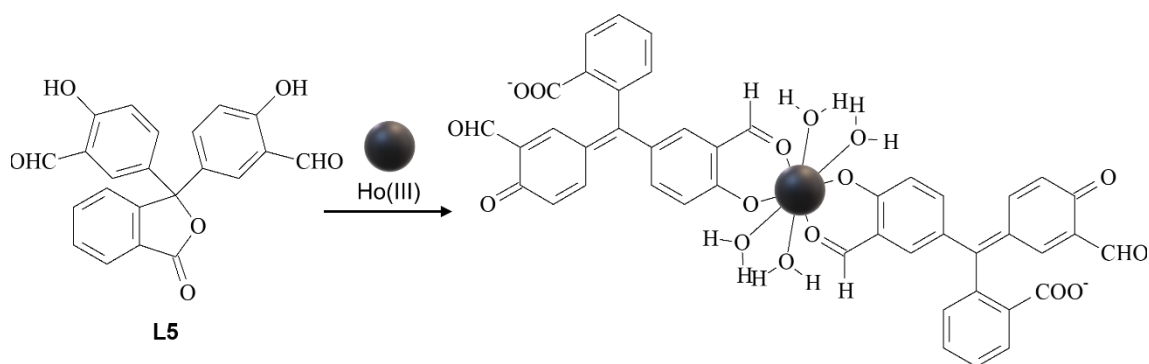
Dubonosov *et al.* reported a series of ligands based on N'-[[4,7-dimethyl-2,5-dioxo-6-(2-(1,3,3-trimethylindolin-2-ylidene)ethylene)-5,6-dihydro-2H-chromene-8-yl]methylene]arylhydrazides, in which the aryl ring linked to the carbonyl of the hydrazide group consists of 4-bromophenyl (**L4a**), 3-biphenyl (**L4b**), 2-naphthyl (**L4c**) or 2-furyl (**L4d**) moieties (Scheme 4) [28]. This family of receptors shows a strong absorption at $\lambda_{max} = 360$ nm. The addition of Ln(III) nitrate salts to a solution of these ligands in acetonitrile leads to the appearance of a new absorption band in the range $\lambda_{max} = 560-571$ nm, which is accompanied by a visually distinct color change from yellow to violet of the solution. This effect increases in the series La(III)<Pr(III)<Eu(III). The metal ions Gd(III) and Ho(III) show a significantly weaker interaction; in particular Ho(III) does not seem to possess any ionochromic property towards this system. The fluorescence emission is strongly influenced by the addition of lanthanide ions; in fact, a decrease of the fluorescence intensity of the free ligand in the range $\lambda_{em} = 442-491$ nm, depending on the ligand used, together with the appearance of a new strong emission at $\lambda_{em} = 617-645$ nm were observed. The effect on the fluorescence emission depends on the Ln(III), decreasing in the series La(III)>Eu(III)>Pr(III)>Gd(III)>Ho(III).



Scheme 4. Structures of **L4a**, **L4b**, **L4c** and **L4d**

Yin *et al.* reported a molecular probe useful to sense Ho(III) over the other REE ions; it is able to switch-on the fluorescence emission resulting also suitable for the localization of Ho(III) in biological systems [29]. The need for holmium sensing arises both from its relative abundance (20 times higher than silver) and from the growing number of uses such as catalyst, glass polisher and in biological applications. Ho(III) exhibits a high affinity for the Ca(II)-binding sites of biomolecules and its bioaccumulation in the body increases the risk of liver diseases; moreover, holmium also expresses its toxicity at the cell membrane level in water animals, damaging it. Sensor **L5** (Scheme 5) bases its photochemical activity on an aldehyde derivative of phenolphthalein and its UV-Vis and fluorescence studies were carried out in buffered water (HEPES)/DMF 1:1 (v/v, pH=7.4) solution. Under these experimental conditions, the free probe is weakly fluorescent displaying low emission at $\lambda_{em} = 480$ nm. Upon the addition of increasing amount of Ho(III) ion, an intense emission band at $\lambda_{em} = 480$ nm appears ($\lambda_{ex} = 365$ nm), whose intensity increases along with the Ho(III) concentration. The fluorescence enhancement could be attributed to the lactone ring-opening caused by the Ho(III) coordination; in fact, the hydroxyl and aldehyde groups coordinate the lanthanide ions, promoting the ring-opening that in turn increases the conjugation of the molecule, making it strongly

fluorescent. MS-ESI studies revealed the presence of a Ho(III) complex with 2:1 ligand to Ho(III) ratio. The ability of the probe to signal the presence of Ho(III) in living cells has been confirmed on HepG2 cells using confocal fluorescence imaging, monitoring the optical window at the yellow channel (450-550 nm). Green fluorescence was observed when the cells were incubated first with the probe and then with HoCl₃ at 37 °C, highlighting the possibility to use **L5** for Ho(III) detection in living systems.



Scheme 5. Structure of **L5** and the proposed mechanism to explain the lactone ring-opening caused by the Ho(III) coordination

4. PURE-LIGAND EMISSION SENSORS

In this section are reported some examples of fluorescent chemosensors in which the coordination of a suitable REE metal ion causes a variation of emission intensity or emission wavelength attributable only to the ligand electronic states. In these systems, the sensing is based on the change of the fluorescence emission with respect to the free

chemosensor. In particular, the coordination of the metal ion affects the emission either increasing or decreasing it; this change can be also accompanied by a shift of the emission wavelength, which can indifferently be towards higher or lower energies. Looking at the quantum yield, if the coordination enhances the emission, the phenomenon is highlighted as CHEF (Chelation Enhancement of Fluorescence effect); on the contrary, the observed emission quenching results as CHQF (Chelation Quenching of Fluorescence effect) [30]. The signal transduction is generally attributed to one or more fundamental mechanisms like the Photoinduced Electron Transfer (PET), the Energy Transfer (ET) or the Twisted Intramolecular Charge Transfer (TICT).

One of the main phenomena exploited by these systems is PET (Photoinduced Electron Transfer). It is related to a red-ox reaction occurring in the overall system in the excited state; commonly, it implicates the excited state of the fluorophore and another moiety of the molecular system, able to perform an electron exchange between them. The explanation of this process lies in the different properties exhibited by the species in their excited or ground states.

The excited state is an unstable energy level showing higher red-ox properties with respect to the ground state. In fluorescent PET-mediated chemosensors, it is the presence of a lone pair on the closest donor atoms that gives the PET; in fact, following the absorption of a photon, an electron of a lone pair on N, O, S or P relaxes to the electronic level of the excited fluorophore occupied by only one electron (ex HOMO) producing an overall non radiative decay (see Figure 6). For this reason, PET is a quenching mechanism for a fluorophore and its impediment, caused by the presence of the metal ion, gives rise to a photochemical response suitable to sense the metal ion itself. In fact, the interaction between chemosensor and metal ion, occurring *via* the lone pair of the donor atom giving

the PET, stabilizes the lone pair energy thus impeding the PET and allowing the fluorescence relaxation (Figure 6). As can be observed, the PET effect does not affect the emission wavelength of the chemosensor but only its fluorescent quantum yield, which usually increases upon the metal ion coordination.

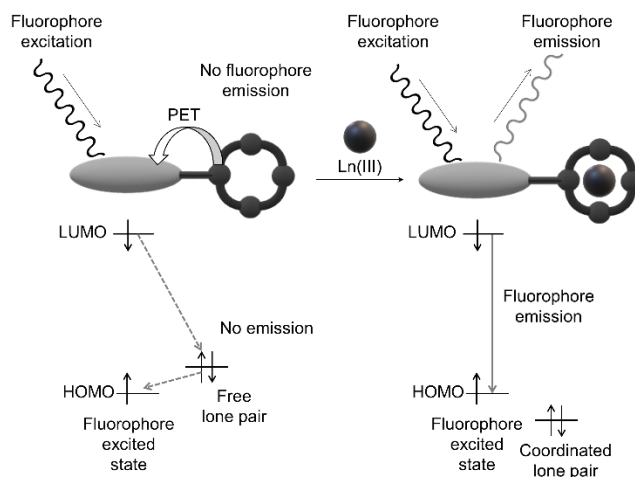


Figure 6. Scheme of PET-effect and simplified orbital diagram

Energy Transfer (ET) is on the basis of the "antenna effect" already described in the section 1 of this review; it consists in the access to an excited f-state of the metal ion due to energy transfer from an excited state of the fluorophore. Nevertheless, the coordination of solvent molecules can affect the emission when they exhibit vibrational states of high energy, as water molecules do; thus, the coordination of water molecules usually produces the quenching of the Ln(III) emission.

For this reason, the coordination of Ln(III) ions to a fluorophore in aqueous solution typically corresponds to a CHQF effect (Figure 7).

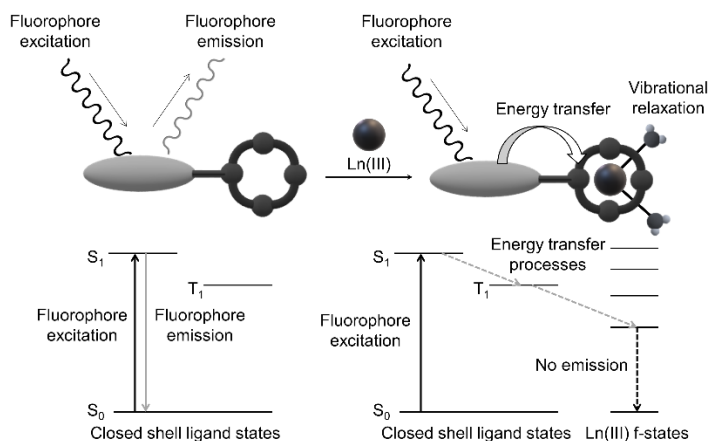


Figure 7. Scheme of the quenching process due to ET and simplified Jablonsky diagram

Twisted Intramolecular Charge Transfer (TICT) is a photoexcitation promoted electron transfer process that occurs in molecules with a single bond separating the donor and acceptor part. Following intramolecular twisting, the TICT state returns to the ground state either through red-shifted emission or by non-radiative relaxation [31].

The free rotation of the free ligand can be hampered by the coordination of the metal ion; TICT based chemosensors are designed in order to be switched-on by the coordination of the suitable metal ion. In fact, the presence of the bound metal ion locks the free rotation of the ligand connecting the donor to the acceptor part of the fluorophore (Figure 8).

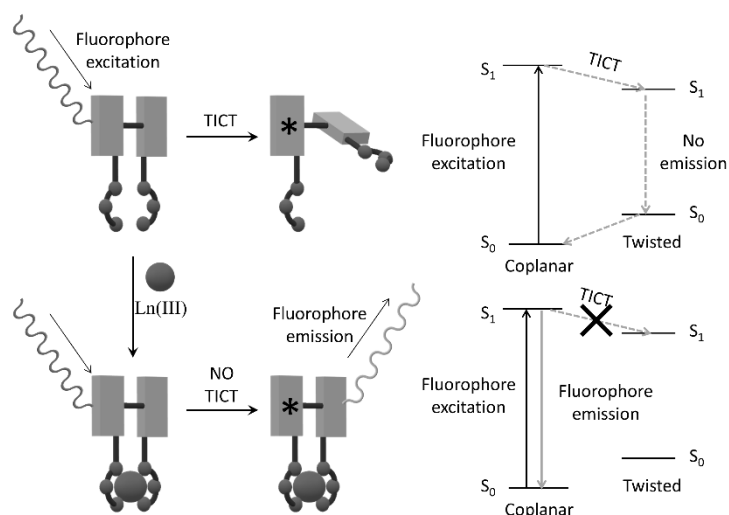


Figure 8. Scheme of the TICT effect and simplified Jablonsky diagram

Faridbod *et al.* reported the synthesis and the fluorescence study on N-[3-methyl-2-(pyridine-2-amido)phenyl]pyridine-2-carboxamide (**L6**) (Scheme 6); the Authors demonstrated that **L6** is able to signal the presence of Lu(III) in aqueous solution by increasing the fluorescent emission [32]. The increasing importance in detecting lutetium, mainly for its recovery, consists, as already mentioned in the introduction chapter, in its presence in many technical or medical devices as well as in fluorescent lamps with low power consumption. Its presence in the environment is growing due to improper disposal of such household waste. Fluorescent emission of **L6** doubles upon Lu(III) ion addition in ethanol-water solution 1:9 (v/v). The increase of the emission is attributed to the formation of a stable **L6**-Lu(III) complex resulting in a binding constant of $\log K = 6.3$ (Table 2); the formation of the complex causes the shift of the emission band from $\lambda_{em} = 462$ nm to $\lambda_{em} = 450$ nm ($\lambda_{ex} = 344$ nm). The emission is due to the whole conjugated system constituted by three aromatic rings and two amide functions. The excited state is of Intramolecular Charge Transfer type (ICT) in which the phenyl group acts as

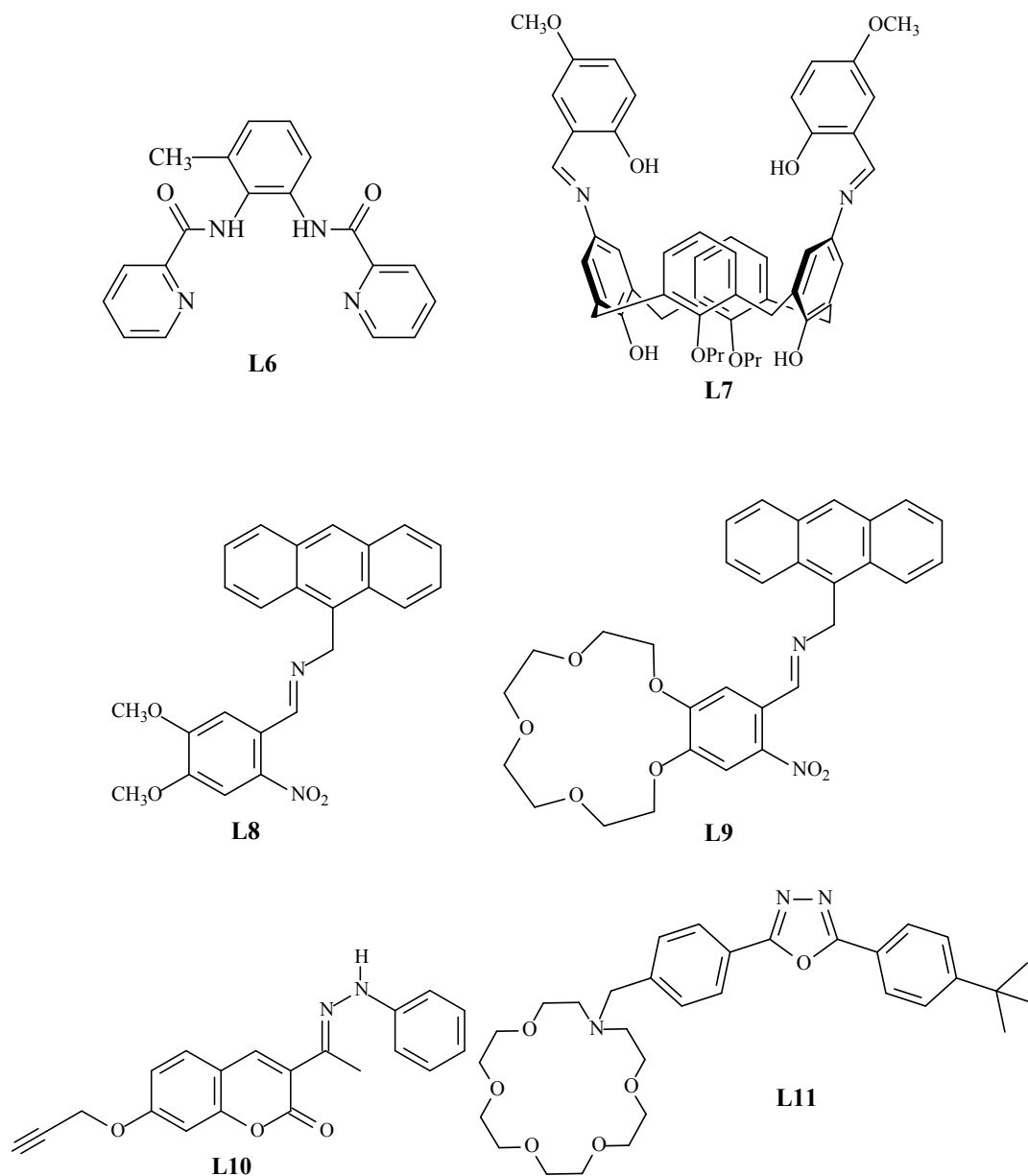
electron-donor towards the two pyridine groups. The blue shift of the emission of the ligand upon Lu(III) coordination suggests that the metal ion perturbs the polarity of the excited state. Authors do not express any explicit hypothesis about the coordination mode but, being the Lu(III) a hard metal ion, most probably it is coordinated by the N-pyridine and the oxygen atom of the amides, leading to the interruption of the conjugation thus explaining both phenomena, namely the blue-shift and the enhancement of the emission intensity due to ICT and PET inhibition, respectively. **L6** can be used for the determination of Lu(III) ion in a concentration range of $3.3 \cdot 10^{-7}$ to $1.0 \cdot 10^{-5}$ mol·dm⁻³ and it was successfully applied in the analysis of Lu(III) enriched water samples.

Gao *et al.* synthesized a diamino-calix[4]arene derivatized with 4-methoxysalicylaldehyde giving the Schiff-base 5,11-bis(2-hydroxy-5-methoxyphenylmethyleneimino)-26,28-dihydroxy-25,27-dipropoxycalix[4]arene (**L7**) (Scheme 6) [33].

The ligand shows two emission bands at $\lambda_{em} = 430$ and 550 nm ($\lambda_{ex} = 375$ nm) in dichloromethane, with the former being much more intense than the latter. Upon addition of Dy(III) or Er(III) the absorption band at 375 nm decreases and a new broad absorption band appears at 450 - 550 nm. In this solvent, the solution containing the ligand is colorless, upon the addition of Dy(III) the color immediately changes to pink, while upon the addition of Er(III) the color changes to yellow after standing in the dark for 24 h. The addition of both Dy(III) or Er(III) causes a drop of the fluorescence band at $\lambda_{em} = 430$ nm while a large CHEF of the band at lower energy, also displacing from 550 to about 600 nm, was observed. Other lanthanides tested, such as La(III), Pr(III), Eu(III), Gd(III) and Yb(III), do not change neither the absorption nor the emission spectra. The reason for such selectivity towards Dy(III) and Er(III) over the other ions could be ascribed to the size-fit effect of the calix[4]arene cavity; it allows these metal ions to be strongly

coordinated by both the imine nitrogen atoms, preventing the PET effect and extending the π conjugate systems, thus accounting for the red shift observed in absorption and emission spectra.

Another example of PET-regulated chemosensor for rare earth ions has been described by Dubosonov *et al.* [34] Ligands **L8** and **L9** (Scheme 6) are dialkoxy-substituted azomethines exhibiting chemosensor activity towards lanthanide cations as well as fluoride, cyanide and acetate anions. In particular, N-[(anthracen-9-yl)methyl]-1-(4,5-dimethoxy-2-nitrophenyl)methanimine (**L8**) is a highly effective sensor for the Eu(III) cation, showing a 25-fold increase of the emission intensity at $\lambda_{em} = 415$ nm ($\lambda_{ex} = 355$ nm) upon its addition in acetonitrile solution. Macrocyclic ligand 4-[N-[(anthracen-9-yl)methyl]methanimine]-5-nitrobenzo-15-crown (**L9**) undergoes only a 8.7-fold increase of the emission. The selectivity towards Eu(III) for both ligands has been demonstrated through competition experiments with other selected REE ions, such as La(III), Nd(III), Sm(III), Tb(III), Dy(III), Ho(III) and Yb(III), transition metal ions such as Zn(II), Cu(II), Co(II) and Hg(II) and, in the case of the crown ether **L9**, with alkali and alkaline-earth metal ions.



Scheme 6. Structures of **L6-11**

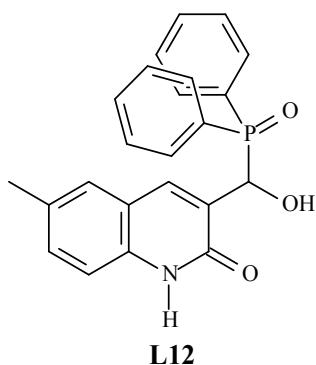
Li *et al.* synthesized the coumarin-based sensor **L10** (Scheme 6) able to selectively detect the Ce(III) ion in aqueous solution [35]. The sensor shows a very weak fluorescence at $\lambda_{em} = 375$ nm in 0.1 mol·dm⁻³ HEPES buffer in EtOH/H₂O (9:1, v/v), pH = 7.2. The addition of Ce(III) induces a drastic enhancement of the fluorescence, with the emission band centered at $\lambda_{em} = 350$ nm. Interestingly, this behavior was observed only with the

Ce(III) ion; in fact, the addition of other lanthanide metal ions such as Pr(III), Yb(III), Nd(III) and La(III) did not cause any distinct change in the fluorescence emission. The detection limit of Ce(III) was estimated to be $2.07 \cdot 10^{-7} \text{ mol} \cdot \text{dm}^{-3}$. The Authors proposed as a possible mechanism for the fluorescence enhancement the inhibition of PET from the nitrogen lone pair to the coumarin fluorophore upon complexation of the metal ion.

Yu *et al.* reported a fluorescent chemosensor in which a monoaza-18-crown-6 is linked to a diaryl[1,3,4]oxadiazole fluorophore by a methylene spacer (**L11**) (scheme 6) [36]. In acetonitrile solution, this sensor shows an emission band at $\lambda_{\text{em}} = 358 \text{ nm}$ that enhances several folds in the presence of REE ions; the order of emission enhancement is $\text{La(III)} > \text{Gd(III)} > \text{Sc(III)} \approx \text{Yb(III)} > \text{Pr(III)} \approx \text{Tb(III)} > \text{Lu(III)} \gg \text{Sm(III)}$. However, the addition of Eu(III) and Ce(III) induces a quenching of the fluorescence, with the highest quenching efficiency observed for Ce(III). This effect allows distinguishing, to a certain extent, Eu(III) and Ce(III) from other REE ions. The 1:1 complexation stoichiometry confirmed that the cavity of the aza-18-crown-6 could host one Ln(III) ion.

Kumar *et al.* reported a quinolone-based system, namely P-[(6-methyl-2-quinolone-3-yl)hydroxymethyl]diphenylphosphine oxide (**L12**) (Scheme 7), able to selectively recognize Lu(III) ion in hydroalcoholic media through enhancement of fluorescence emission (CHEF) [37]. In water-methanol 1:1 solution this ligand shows a weak emission at about $\lambda_{\text{em}} = 400 \text{ nm}$ ($\Phi = 0.063$, $\lambda_{\text{ex}} = 280 \text{ nm}$) that doubles in intensity ($\Phi = 0.118$) upon the coordination of Lu(III); the limit of detection is about 25 nM, much lower than the WHO guidelines for drinking water for Lu(III) (76 μM). This sensor can work in a wide pH range, from 4.0 to 9.0. The stoichiometry of the complex formed is $[\text{LuL12}_2]^{3+}$, with formation constants of $\log\beta_{1:1} = 3.14$ and $\log\beta_{1:2} = 5.1$ (Table 2). The other REE ions form similar complexes with $\log\beta_{1:1}$ ranging from 1.08 to 1.96 and $\log\beta_{1:2}$ ranging

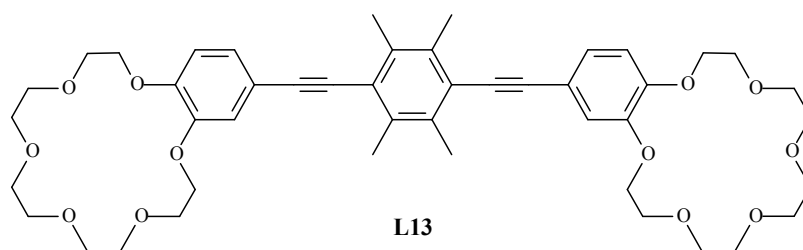
from 2.44 to 2.97, but without any effect on the emission spectrum. Competition experiments demonstrated that the co-presence of other metal ions, such as Ca(II), Al(III), uranyl, transition and REE ions, does not affect the efficiency of the Lu(III) sensing. Authors attribute the CHEF effect to the increase of the ligand rigidity upon metal ion complexation, that prevents the quenching of the fluorescence due to TICT paradigm.



Scheme 7. Structure of **L12**

In many cases, the energy transfer from the excited state of the ligand to the lanthanide ion causes the quenching of the fluorescence and this occurs when the excited lanthanide ion decays with a non-radiative pathway. For example, as already mentioned, the coordination of water molecules to the metal center quenches the emission of the Ln(III) complexes. Schmehl *et al.* reported the ditopic ligand 1,4-bis(3'-ethynylbenzo-18-crown-6)-2,3,5,6-tetramethylbenzene (**L13**) (Scheme 8), that is luminescent; the coordination of lanthanide ions with larger dimensions and showing f-f transitions, such as Pr(III) and Nd(III), quenches the emission [38]. Alkali, alkaline-earth and lanthanide ions with smaller radii such as Gd(III), Tb(III), Dy(III) and Yb(III) do not affect the emission. The experiments were carried out in acetonitrile solution, where the free ligand shows an intense emission band centered at $\lambda_{em} = 406$ nm ($\lambda_{ex} = 340$ nm, $\Phi = 0.67$). The addition

of Pr(III) or Nd(III) induces a blue shift of the fluorescence maximum and the intensity is significantly reduced of 65% and 61%, respectively. In contrast, the addition of other lanthanide ions such as Dy(III), La(III), Tb(III) and Yb(III), leads to a similar blue-shift of the emission band but without significantly quenching the fluorescence (reduction of 15% for Dy(III) and less of 5% for Tb(III)). A possible explanation of the emission quenching could be an energy transfer promoting excited states of the lanthanide ion by either exchange or coulomb processes, namely the excited state of the ligand transfers the energy towards the lanthanide ion, that vibrationally decays due to the coordinated water molecules. The lanthanide f-f emission is not observed.



Scheme 8. Structure of **L13**

Table 2. Logarithm of the equilibrium constants ($\log \beta$) of selected ligands for REE complexation.

	L1	L2	L3	L4	L5	L6	L7	L12
La(III)	36.42 ^a	-	nd ^b	5.14 ^b	-	-	-	-
Ce(III)	-	-	-	-	-	-	-	-
Pr(III)	-	-	nd ^b	-	-	-	-	-
Nd(III)	-	-	-	-	-	-	-	-
Eu(III)	35.24 ^a	7.57 ^b	5.14 ^b	-	-	-	-	-
Gd(III)	-	-	nd ^b	-	-	-	-	-
Tb(III)	35.23 ^a	4.33 ^b	-	-	-	-	-	-
Dy(III)	-	-	nd ^b	-	7.03 ^c	-	5.41 ^c	-
Er(III)	35.76 ^a	-	nd ^b	-	-	-	5.77 ^c	-
Yb(III)	-	-	nd ^b	-	-	-	-	-
Lu(III)	-	-	-	-	-	6.3 ^d	-	3.14 (1:1)* ^g 5.1 (1:2)

^a water, ^b acetonitrile, ^c water/DMF 1:1, ^d ethanol/water 1:9, ^e dichloromethane, ^f ethanol/water (HEPES) 9:1, ^g water/methanol 1:1.

nd: not determined.

*: 1:1 = LuL12, 1:2 = Lu(L12)₂.

5. BIO-ENGINEERED FLUORESCENT SENSORS

Nature uses a large number of biosensors capable of detecting and remediating toxic metal ions present in the environment as contaminants. In this context, many bacteria, in order to respond to environmental changes, rely primarily to two-component signal transduction systems consisting of a histidine-based sensor and a response regulator. This class of biosensors generally acts through the regulation of a specific kinase activity; in fact, the insertion of a phosphate group in an appropriate position of a protein represents the molecular output of the interaction with a guest species. The detection of a specific signal activates the sensor kinase leading to autophosphorylation of a highly conserved histidine residue; the phosphate group is then transferred to a conserved aspartate residue in the coupled regulator protein, which, in turn, activates or represses the transcription of

suitable target genes. An important example is the PmrA/PmrB two component system found in *Salmonella* species, that responds to extracellular Fe(III) ion. PmrB is a transmembrane protein of about 350 residues, both N- and C-terminals are inside the cell while a loop of about 30 amino-acids is situated at the external side of the membrane and forms the Fe(III) specific receptor. Recently, He *et al.* engineered artificial sensors in *E. coli* based on a modified PmrA/PmrB system in which the Fe(III) domain has been substituted by lanthanide-binding tags (LBT) [39], previously reported by Imperiali *et al.*, able to bind lanthanide ions not only with high affinities, but also in a selective way [40]. Authors constructed a PmrA/PmrB-responsive system bearing the plasmid pJBA25-*pmrC* in which the phosphorylation of PmrA activates a *pmrC* promoter fused to the *gfp* gene, encoding for a green-fluorescent protein (GFP). This engineered *E. coli* is able to detect Tb(III) ion with a fluorescent response. Upon Tb(III) binding to the LBT sequence, an elongation of the transmembrane domain of PmrB unit due to the folding of the loop was observed; this carries the signal for the auto-His phosphorylation that then phosphorylates PmrA. The phosphorylated PmrA, interacting with the *pmrC* promoter, activates the transcription of a gene encoding for the green-fluorescent protein (Figure 9). Engineered *E. coli* has been tested measuring their fluorescence emission at $\lambda_{em} = 520$ nm ($\lambda_{ex} = 485$ nm). The presence of Fe(III) (100 μ M), Cu(II) (10 μ M), Mn(II) (20 μ M), Zn(II) (10 μ M) or Ca(II) (10 μ M) does not significantly affect the underground emission intensity, while the presence of Tb(III) at the concentration of 1.0 μ M triplicates the emission intensity. The system can be considered the first example of engineered sensory bio-system based on the bacterial response exploited to sense lanthanide ions.

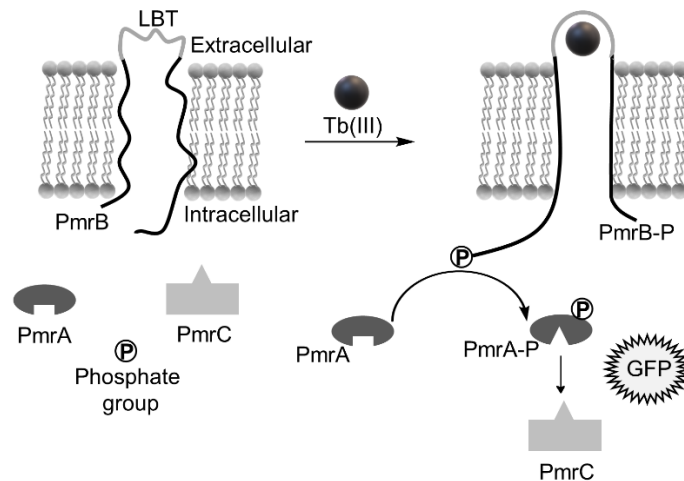


Figure 9. Scheme of the engineered bio-system able to respond to the presence of lanthanides. It is based on modified PmrA/PmrB proteins, consisting of the histidine kinase PmrB and the responding regulator PmrA, acting on the *pmrC* promoter fused to the *gfp* gene. Binding of Tb(III) ion by LBT sequence in PmrB activates its auto-phosphorylation which subsequently phosphorylates PmrA. This latter activates the *pmrC* promoter inducing the synthesis of a green fluorescent protein (GFP)

Cotruvo *et al.* engineered a protein-based fluorescent sensor able to detect REE ions at the nanomolar level by derivatizing lanmodulin [41]. Lanmodulin is a high-affinity lanthanide binding protein recently identified in *Methylobacterium extroquens*, a bacterium that needs lanthanides to make two enzymes work. This protein possesses four EF-hands, namely metal coordination motifs generally associated with Ca(II) binding, but it shows a 10^8 -fold higher selectivity for Ln(III) and Y(III) than for Ca(II) (Figure 10) [42,43].

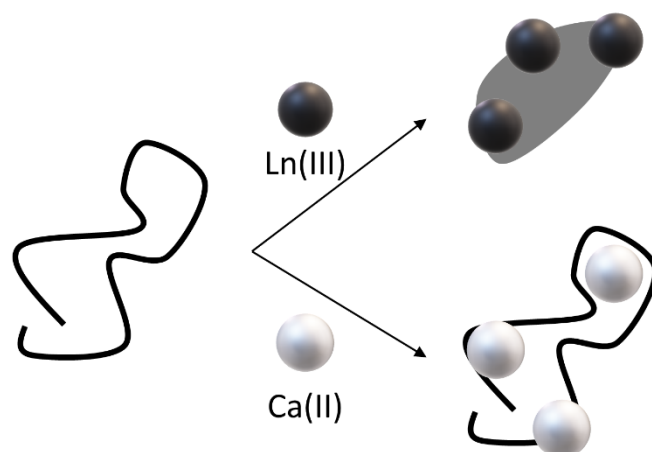


Figure 10. Schematic drawing of LaMPI biosensor response to Ln(III) with 100 million-fold selectivity over Ca(II)

Taking advantage from the previous work of Tsien *et al.* on calmodulin [44], the Authors engineered the new LaMPI biosensor, namely a lanmodulin derivative including two fluorescent proteins able to obtain the Foster resonance energy transfer effect. The two inserted proteins were the C-terminally truncated enhanced cyan fluorescent protein (ECFP) and the yellow fluorescent citrine. The obtained fluorescence effect is also called FRET (Fluorescence Resonance Energy Transfer) and it necessitates of a pair of different fluorescence emitters. This because FRET is a phenomenon consisting in the energy transfer from a fluorophore to another provoking the photon emission of this latter; the effect is affected by the distance between the two fluorophores. The energy of the excited transferring fluorophore is dissipated by exciting the second one without photon emission; in other words, the first fluorophore, in its excited state, decays by photons emission which are captured by the second one thus giving an energy transfer from the first fluorophore to the second one; the latter finally emits photons, which possess lower energy than the previous ones. Therefore, the phenomenon consists in exciting one of the

two fluorophores to obtain the fluorescent emission of the second one. The conditions to observe the FRET effect are mainly three: *i*) the two donor and acceptor fluorophores must be in close proximity (usually 10–100 Å); *ii*) the fluorescence emission energies of the donor must be in the same range of the absorption energies of the acceptor (the emission spectra of the donor must overlap with the absorption spectra of the acceptor); *iii*) the orientation of the transition dipoles between donor and acceptor have to be as much as possible parallel. The efficiency of FRET depends on $1/d^6$, where d is the intermolecular separation between the two fragments. LaMPI is able to link three Ln(III) ions undergoing a conformational change that brings ECFP and citrine close to each other allowing for FRET (Figure 11). Upon excitation at $\lambda_{\text{ex}} = 433$ nm, free LaMPI exhibits two emission bands at $\lambda_{\text{em}} = 475$ nm (ECFP) and $\lambda_{\text{em}} = 529$ nm (citrine); when Ln(III) ions are added, the band at $\lambda_{\text{em}} = 475$ nm decreases while that at $\lambda_{\text{em}} = 529$ nm increases in intensity, LaMPI behaving as a ratiometric fluorescence sensor. The FRET response is the ratio between the emission intensity at $\lambda_{\text{em}} = 529$ nm and that at $\lambda_{\text{em}} = 475$ nm. This system showed a ratiometric response to all REE ions by increasing the emission of seven-fold; in addition, the apparent dissociation constants for the Ln(III) and Y(III) systems are in the picomolar range, thus only 2-fold weaker than those of native lanmodulin. LaMPI also exhibits fluorescence response to Ca(II) with an apparent dissociation constant in the millimolar range, far above physiological levels, and a FRET response of only 3-fold. At the end, the Authors tested the LaMPI response versus other common trivalent and divalent metal ions such as Al(III), Fe(III) and Mn(II), Cu(II), exploring concentration ranges potentially relevant to aqueous environment, finding little or no fluorescence response.

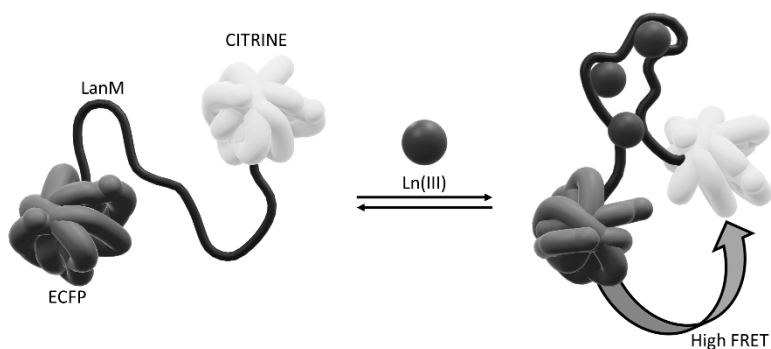


Figure 11. Signal transduction mechanism of the LaMPI biosensor proposed by Cutruvo *et al.* When three Ln(III) ions bind to the lanmodulin chain (LanM), a conformational change occurs bringing enhanced cyan fluorescent protein (ECFP, $\lambda_{\text{ex}} = 433 \text{ nm}$, $\lambda_{\text{em}} = 475 \text{ nm}$) and citrine ($\lambda_{\text{em}} = 529 \text{ nm}$) close to each other, allowing for FRET

6. FLUORESCENT SUPRAMOLECULAR SYSTEMS AND NANOMATERIALS

In this section, a selection of the many fluorescent chemosensors for REE ions based on supramolecular aggregates or nanoparticles are described. An advantage of the use of aggregates or nanoparticles to build chemosensors is the possibility both to enhance the fluorescence signal loading the particles with high concentrations of dyes, as well as to realize sensor-arrays including into the system several chemosensors with different response towards different chemical species.

Ding *et al.* developed a sensor system basing its response on an aqueous mixture containing bispyrene derivatives and a surfactant (sodium dodecyl sulfate, SDS) able to dissolve the otherwise insoluble organic chemosensor in water; in this way, the chemosensors are able to discriminate lanthanide ions in aqueous solution. The system is constituted by three cationic bis-pyrene derivatives (**L14a**, **b** and **c**) (Figure 12) mixed with the anionic surfactant (SDS); **L14a-c** show two pyrene-imidazol fluorescent

fragments spaced together by alkyl chains of different length [45]. The system can emit fluorescence of different wavelengths caused by each fluorescent pyren-imidazol fragment and by the formation of an excimer when the two fragments are close one to another. The spectra obtained are the outcome of these emissions and their change can be related to the presence of the lanthanide ions in the medium, thus furnishing the response useful for their recognition. It has to be considered that the spectra contain six-emission signals giving a specific pattern for each lanthanide ion. The output data mathematically elaborated with the principal component analysis (PCA) method give the possibility to recognize 6 ions of the lanthanide series, namely La(III), Pr(III), Nd(III), Eu(III), Ho(III) and Er(III). On the basis of in-depth studies carried out to monitor the behavior of micelles containing the single bis-pyrene sensors **L14a**, **b** and **c**, obtained with SDS or a non-ionic surfactant (Tween 80), and taking into account that divalent ions find no response, the Authors deduced that the strong electrostatic interaction between hard Ln(III) cations and the highly negative charged surface of micelles is responsible for the multiple fluorescence response.

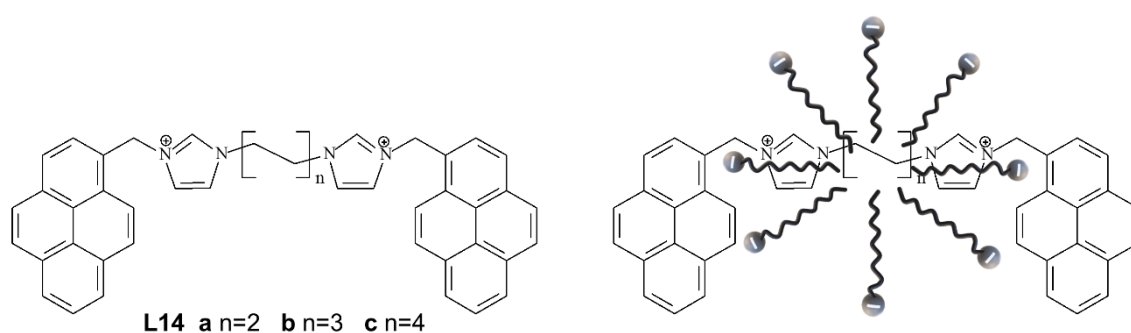


Figure 12. Representation of the micelles loaded with ligands **L14a-c** reported by Ding *et al.*

A nano-structured material that has been used in many applications for chemical sensors is Graphene, and in particular Graphene oxide (GO). GO has a singular photoluminescence emission pattern due to the presence of various oxygenated functional groups (epoxide, carbonyl, carboxyl) and other oxidized sp^3 sites that contributes to the band gap typical of this material. In particular, the control of the sp^2 domain in the sp^3 matrix of GO can be used to tune both fluorescence intensity and emission wavelength [46,47].

Faridbod *et al.* utilized graphene quantum dots (GQDs) able to selectively signal Ce(III) in water; the system is based on a chemosensor of nano-dimension resulted very efficient in the Ce(III)-sensing [48]. GQDs are synthesized starting by graphite powder through a top-down approach and they have a diameter mainly distributed in the range of 15–20 nm. Due to the oxidative process used in the synthesis of GQDs, oxygen-containing functional groups, including carbonyl/carboxylate, hydroxyl and epoxide groups, are introduced at the edge and on the basal plane of the nanoparticles. The GQDs exhibit a high fluorescence emission centered at 440 nm wavelength ($\lambda_{ex} = 335$ nm). The emission quenches upon the addition of Ce(III) ions but is not influenced by other REE or transition metal ions (Figure 13). The mechanism related to the quenching mechanism has been attributed to the red-ox properties of Ce(III), considering that Ce(III) is the easiest oxidable ion among all M(III) ions of the series, leading to the Ce(IV) oxidation state; thus, it is the only one able to reduce some organic groups located on the quantum dot surface. This red-ox reaction affects the emission of GQDs giving a response to the presence of Ce(III) by quenching it.

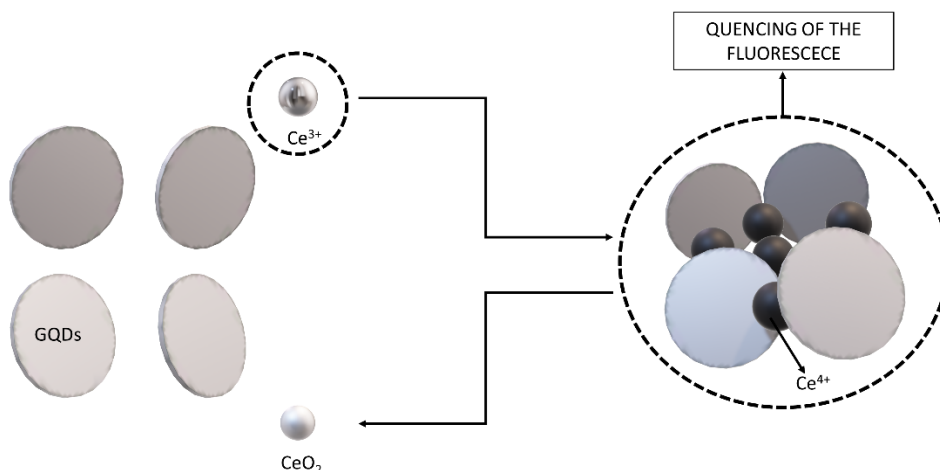


Figure 13. Schematic illustration of the selective detection of Ce(III) by graphene quantum dots (GQDs): among all metal ions tested, the fluorescence intensity of GQDs is quenched only by addition of Ce(III)

Nandhakumar *et al.* realized a new graphene oxide-resorcinol hybrid material (GO-R) able to detect Ce(III) ions in aqueous environment [49]. GO-R hybrid nanoparticles consist in GO sheets with resorcinol strongly adsorbed on their surface. They show a characteristic emission band at $\lambda_{em} = 306$ nm ($\lambda_{ex} = 273$ nm). The addition of Ce(III) increases the fluorescence intensity at $\lambda_{em} = 306$ nm together with the growing of a new band centered at 351 nm. Authors explained this behavior by suggesting the occurrence of ICT between graphene oxide and resorcinol, favored by the presence of the metal ion. Competition experiments have demonstrated that interfering metal ions leave the emission of the system unchanged, thus the GO-R receptor could be employed in real matrices for the selective detection of Ce(III) (Figure 14).

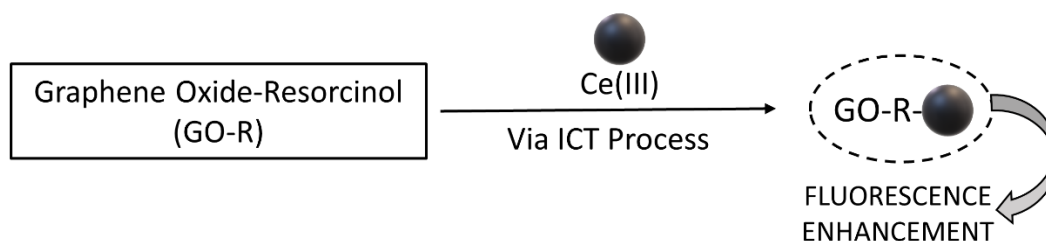


Figure 14. Schematic illustration of the selective enhancement of fluorescence of graphene oxide- Resorcinol hybrid material (GO-R) in the presence of Ce(III) ions

Another class of photoactive nanoparticles are Quantum Dots (QDs). QDs are semiconductors nanocrystals composed by the combination of elements of the 12th and 16th groups (eg. CdSe, CdTe, CdS or ZnSe) or 13th and 15th groups (eg. InP or InAs), displaying peculiar optical, electrical, magnetic and catalytic properties. Regarding the optical properties they have a narrow emission band with high quantum yield ($\Phi_{em} = 0.2-0.9$), thus appropriately derivatized QDs are extensively used as luminescent probes for the detection of various analytes like metal ions, anions and organic molecules [50-52]. Rofouei *et al.* reported on glycine dithiocarbamate (GDTC)-functionalized manganese doped ZnS Quantum Dots (GDTC-Mn:ZnS) (Figure 15) able to selectively recognize Ce(III) ions by fluorescence quenching [53]. The conjugated nanoparticles suspended in PBS solution at pH=7.5 show an intense fluorescence band at $\lambda_{em} = 575$ nm ($\lambda_{ex} = 300$ nm) due to Mn(II) ions incorporated in the QDs and a weak band at $\lambda_{em} = 415$ nm attributed to defect-related emission of ZnS. The addition of Ce(III) causes a Stern-Volmer-type quenching of the band at $\lambda_{em} = 575$ nm. This system shows a detection limit of $2.29 \cdot 10^{-7}$ mol·dm⁻³ and an excellent selectivity for Ce(III) over other competitive REE cations due to the strong affinity of this metal ion towards the GDTC ligand.

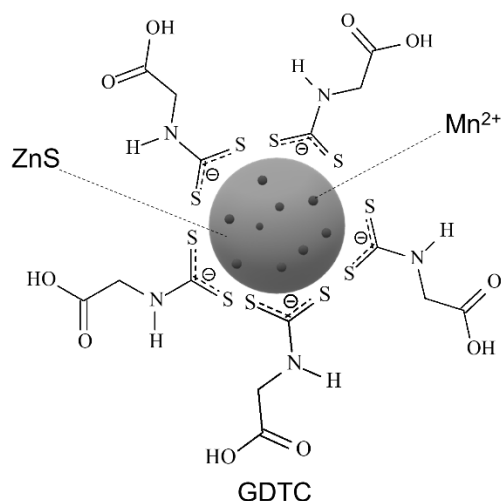


Figure 15. Scheme of the GDTC-Mn:ZnS quantum-dots. A core of luminescent Mn(II)-ZnS doped nanoparticles is covered by glycine dithiocarbamate (GDTC) molecules that act as Ce(III)-binding motive

Chu, Wang *et al.* prepared nitrogen-doped graphene quantum dots (N-CGDs) through a one-step method employing graphene oxide (GO) and subsequent dialysis to obtain a new fluorescent probe for Ce(IV) [54]. These new Graphene quantum dots contain many oxygen functional groups, thanks to them showing a strong blue emission. Fluorescence spectra were obtained exciting at 320 nm a N-GQD aqueous solution (0.015 mg ml^{-1}) and it was possible to observe a strong emission band at 450 nm. The addition of Ce(IV) solutions of increasing concentration (from 0 to $534 \text{ }\mu\text{M}$) showed a gradually decrease in the emission intensity. The calibration of the curve showed a linear range between 1 and $44 \text{ }\mu\text{M}$, suggesting the good sensitivity of the system. To check the selectivity of the sensor, the Authors performed fluorescence studies by mixing $200 \text{ }\mu\text{M}$ of various REE ions solutions (Sc(III), Y(III), La(III), Ce(III), Ce(IV), Pr(III), Nd(III), Sm(III), Eu(III), Gd(III), Tb(III), Dy(III), Ho(III), Er(III), Tm(III), Yb(III) and Lu(III)) with an aqueous solution of N-GQDs and exciting at 320 nm; they observed that only Ce(IV) is able to decrease the signal. The same analysis, carried out on the same samples after the addition

of 200 μM of a solution of Ce(IV), revealed a significant quenching effect confirming the selectivity of the system for this ion (Figure 16). Once again, the intrinsic redox properties of Ce(IV)/Ce(III) ions have been considered at the base of the quenching mechanism. Upon its addition to a solution containing the sensor, Ce(IV) is reduced to Ce(III) that is able to bind to N and O atoms of N-GQDs, thus the new complexes formed lead to agglomeration of the N-GQDs allowing for the fluorescence quenching caused by electron transfer effects.

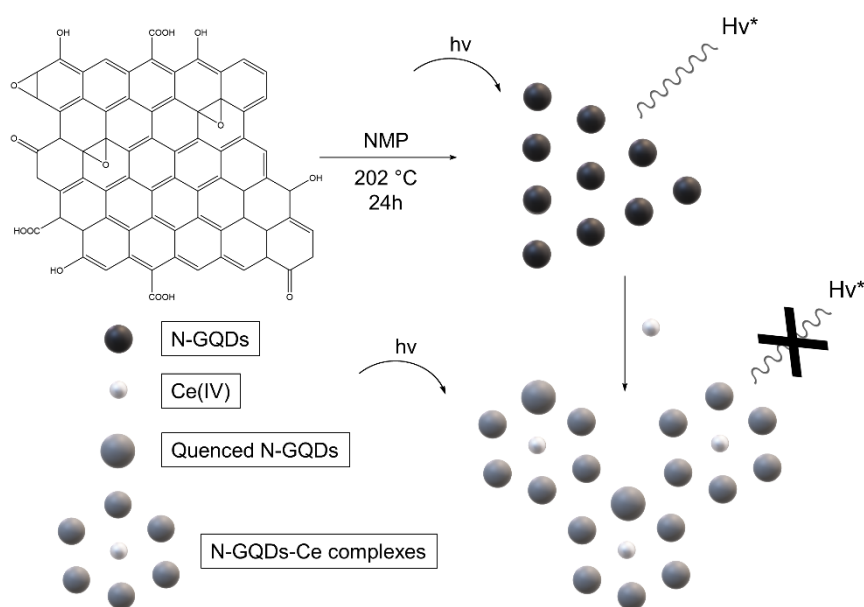


Figure 16. Synthesis of N-GQDs and the possible fluorescence mechanism

A versatile and useful class of nanoparticles suitable for sensing purposes are Carbon Dots (CDs). CDs are a family of nanoparticles with diameter less than 10 nm, based on carbon atoms. CDs show fluorescent properties; they can be easily obtained starting from common reagents using processes of carbonization, usually in an overall low cost procedure. The emission spectra of CDs cover a wide range of wavelengths which are affected by the excitation wavelength and by the close environment, permitting sensing

applications. Noteworthy, CDs retain a sort of structural memory of their organic precursor, endowing the nanoparticles with molecular recognition capability depending on the functional groups of the precursor molecule [55,56].

Jelinek, Paz-Tal *et al.* applied successfully the CDs paradigm realizing a selective fluorescent sensor for Sm(III), Eu(III) and UO_2^{2+} ions based on Carbon Dots-silica aerogel hybrid. They were prepared by in situ carbonization of 2-thenoyltrifluoroacetone (TTA) that is a suitable ligand to bind heavy metal ions (Figure 17) [57].

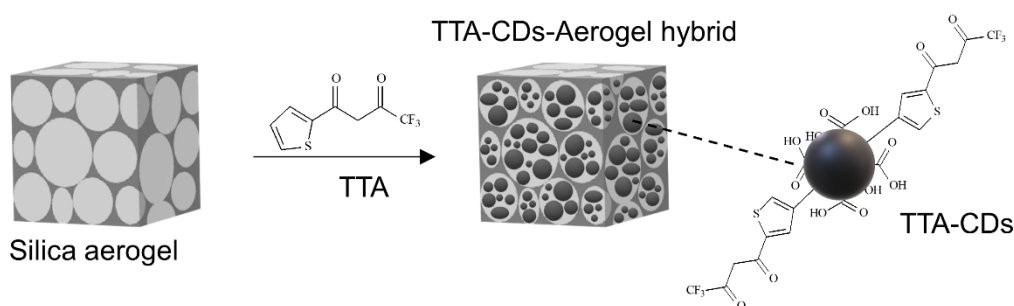


Figure 17. Simplified representation of Carbon Dots-silica aerogel hybrid derived in situ by carbonization of 2-thenoyltrifluoroacetone (TTA).

The sensing material was formed by silica annealing carried out at high temperature and high pressure of nitrogen; the CDs were formed directly in situ, filling the pores of the aerogel with an ether solution of TTA and heating at 140 °C to generate the aerogel-embedded CDs. The emission maximum of the system depends on the selected excitation wavelength; for example, upon excitation at $\lambda_{\text{ex}} = 350$ nm the emission band is centered at $\lambda_{\text{em}} = 405$ nm, while by exciting at $\lambda_{\text{ex}} = 400$ nm the emission band is observable at $\lambda_{\text{em}} = 445$ nm. The addition of UO_2^{2+} , Sm(III) or Eu(III) gives rise to different responses. Uranyl causes a marked red-shift of the emission band at $\lambda_{\text{em}} = 445$ towards 480 nm (λ_{ex}

= 400 nm), while Sm(III) and Eu(III) determine a net quenching of the emission band at $\lambda_{em} = 405$ nm ($\lambda_{ex} = 350$ nm). In this work, Authors highlighted the versatility of the systems obtained to be used for sensing applications of different substrates.

A sensitive fluorescent nano-chemosensor for Eu(III) ion was reported by Hosseini *et al.* [58] It is based on a magnetic core-shell nanoparticle functionalized with cinchonidine (CD) (Figure 18), a natural alkaloid used in asymmetric synthesis in organic chemistry. This system shows a selective interaction with Eu(III) ion. These nanoparticles show a fluorescence band at $\lambda_{em} = 375$ nm ($\lambda_{ex}=330$ nm) that significantly increases in intensity upon addition of growing amounts of Eu(III) ion. Other mono-, di- or trivalent metal ions as Na^+ , Cs^+ , Ca^{2+} , Sr^{2+} , Co^{2+} , Cu^{2+} , Zn^{2+} , Cd^{2+} , Hg^{2+} , Pb^{2+} , Al^{3+} , Cr^{3+} , Ce^{3+} , La^{3+} , Pr^{3+} , Nd^{3+} , Sm^{3+} , Ho^{3+} , Tm^{3+} and Yb^{3+} , cause either weaker changes or no changes in fluorescence intensity and, in competition experiments, they do not influence the response to Eu(III). Authors reported a binding constant of $1.7 \cdot 10^5$ mol \cdot dm $^{-3}$ with a detection limit of $5.0 \cdot 10^{-9}$ mol \cdot dm $^{-3}$.

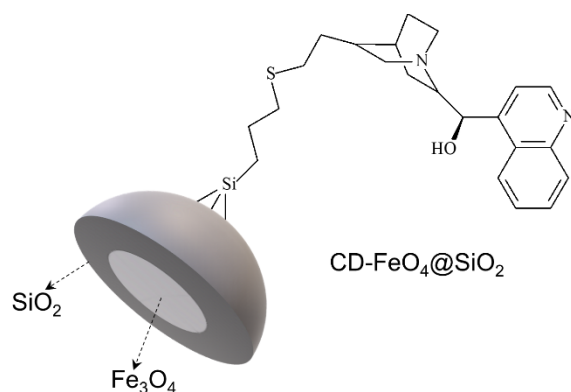


Figure 18. Structure of magnetic core-shell nanoparticles functionalized with cinchonidine (CD) reported by Hosseini *et al.*

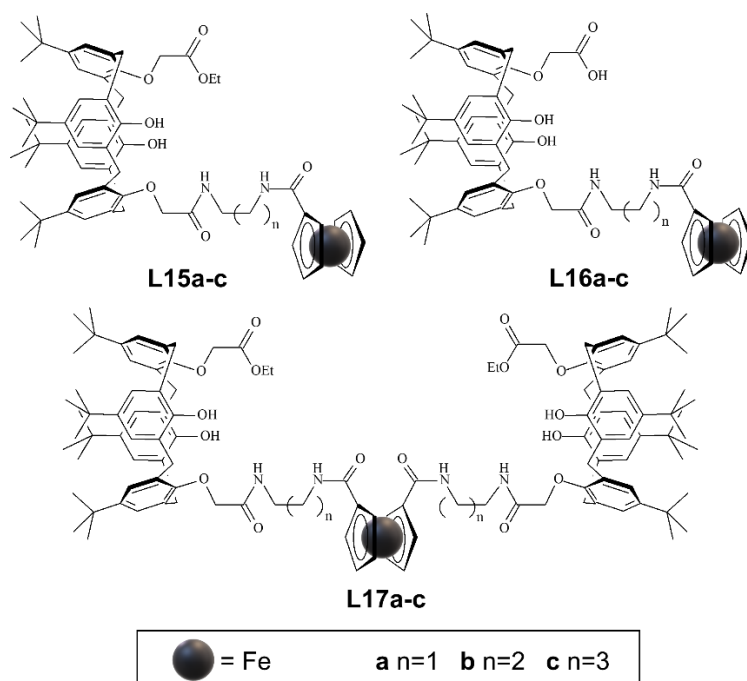
7. ELECTROCHEMICAL SENSORS

In this section, the contribution of the electrochemical sensors is reported. As all the sensors, also those exploiting an electrochemical response must be selective and sensitive to have a response time sufficiently fast and a detection limit sufficiently low as well as a simple calibration method. Moreover, the measurement must be sufficiently reliable, repeatable and easy to perform. Depending on the type of the technique used, the importance of these factors can change [59]. The binding event between analyte and receptor can be effectively monitored and measured by different electrochemical techniques [60]. Voltammetry and potentiometry are techniques that can be applied for the detection of a selected target; both show high sensitivity and an overall quite low-cost also in terms of time consuming. Below are reported some examples of sensors exploiting cyclic voltammetry (CV), square wave voltammetry (SWV) and potentiometry with ion selective electrodes as electrochemical measurement acting through two different approaches.

Regarding the next two examples reported, the first one is a redox-active system, where the coordination of Ln(III) affects the oxidation potential of the receptor, while the second one is a screen-printed electrode modified with a polycathecol-film in order to amplify the voltammetric signal of Eu(III) ion.

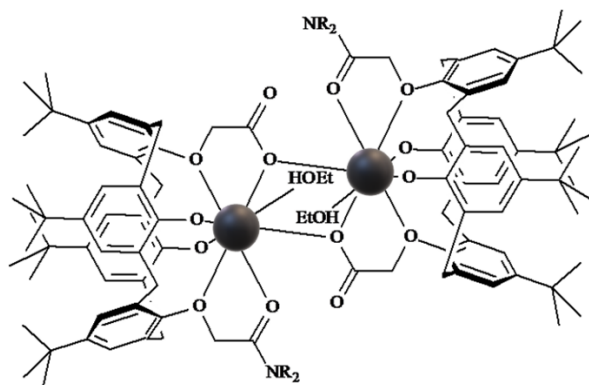
Ferrocene derivatives are among the most used voltammetric probes due to their marked electrochemical properties given by the presence of the redox couple ferrocenium/ferrocene (Fc^+/Fc), whose reduction potential depends on its chemical environment. Beer *et al.* synthesized a series of calix[4]arene macrocycles containing ferrocene units on which, depending on the ligand, further coordinating groups such as

ester, amide and acid groups are present (**L15a-c**, **L16a-c** and **L17a-c**) (Scheme 9) [61]. The calixarene moiety is the binding framework having two or three deprotonable OH groups and at least other three or four hard oxygen functions, while the ferrocene constitutes the sensing electrochemical-active moiety.



Scheme 9. Structures of **L15a-c**, **L16a-c** and **L17a-c**

Preliminary studies on the precursor 5,11,17,23-tetratert-butyl-25-carboxymethoxy-27-dialkylaminocarboxymethoxy-26,28-dihydroxycalix[4]arene (**L18**) highlighted that the calixarene side arm of the ligands can bind Ln(III) ions forming monomeric or dimeric 1:1 complexes (Scheme 10). The formation constants for mononuclear complexes of **L15a-c** and **L16a-c** with Ln(III) ions are in the range of 2.95 to 5.18 logarithm units.



Scheme 10. Structures of $[\text{Eu}_2(\text{H}_3\text{L18})_2(\text{EtOH})_2]$

Analogously, it was possible to observe, through ES-MS studies, the molecular ions corresponding to $[\text{LaH}_2\text{L17c}]^+$, $[\text{GdH}_2\text{L17c}]^+$ and $[\text{LuH}_2\text{L17c}]^+$ species, therefore suggesting the ability of **L17a-c** to coordinate lanthanide ions forming complexes with a 1:1 ligand to metal ratio. Electrochemical studies were performed in acetonitrile solution using CV and SW voltammetry using $0.1 \text{ mol}\cdot\text{dm}^{-3} \text{ NBu}_4\text{BF}_4$, as supporting electrolyte; the data were analysed considering the ferrocene/ferrocenium (Fc/Fc^+) couple, and they were collected at different concentrations of La(III), Gd(III) and Lu(III). All nine ligands showed a single, quasi-reversible oxidation profiles in their cyclic voltammograms and revealed to be stable in the electrochemical conditions used. The reduction signal of ferrocene linked to calixarene is displaced towards cathodic zone of 141-180 mV depending on the ligand structure. Upon the addition of lanthanide ions, a marked anodic shift in the oxidation potentials was observed for all ligands, with the dimeric ligands **L17a-c** undergoing the largest shifts (80-205 mV vs 10-60 mV for **L15a-c** and **L16a-c**). The effect depends on the REE added, the smallest Lu(III) ion causing the highest oxidation potential shift because its smaller ionic radius determines a greater polarization close to the ferrocene unit. The addition of an excess of lanthanide ions does not induces shift, instead the different alkyl chain lengths gave a different effect on the response.

Other metal ions, like sodium and potassium in high concentration, gave a non-significant potential shift. These calixarene ligands resulted suitable to selectively bind lanthanide ions forming mononuclear 1:1 stable complexes. This gave rise to a marked voltammetric response measurable with both CV and SW methods, thus they can be considered efficient electrochemical sensors for lanthanide ions.

Another electrochemical technique consists in the use of specific ion-imprinted electrodes allowing for the detection of the metal ion by Voltammetry. In this contest, Cao *et al.* developed an electrochemical sensor for Eu(III) determination through a modified screen-printed electrode (SPE) [62]. Screen-printed electrodes are easily and rapidly produced and these aspects, together with their low costs, are important for their use in transducers for electrochemical sensors. Screen-printed based electrodes have a big advantage in the possibility to be modified, not only with regard to metal-sensitive film formation, but also by incorporating molecules or nano-size materials. This versatility, together with their miniaturized size, makes them good candidates for on-site determination of target analytes with portable instrumentation, not only in environmental monitoring, but also in food, agricultural and biomedical analysis. It is to consider that the maximum concentration allowed for europium in environmental water is $6 \text{ mg}\cdot\text{dm}^{-3}$, [62] thus the development of selective and sensitive electrode for Eu(III) determination is an interesting challenge. To improve the sensitivity and the selectivity of the electrochemical sensors towards Eu(III), the Authors fabricated a working electrode using a SPE as substrates electrode, a signal amplifying based on poly-catechol (PC) film and an Eu(III) ion-imprinted membrane as the recognition unit. The presence of the hydroxyl groups of the catechol revealed to be a key choice to increase the sensor sensitivity as these groups can coordinate Eu(III) ions. The modified Eu(III)-IIM/PC/SPE electrode was prepared

covering a SPE electrode, constituted by a first layer of electropolymerized PC and a second layer of Eu(III)-imprinted silica gel (Figure 19).

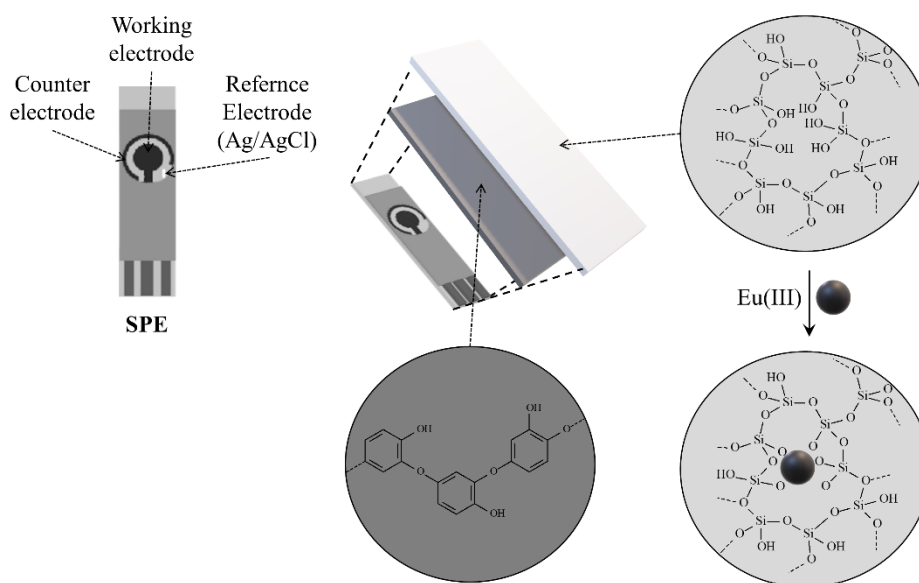


Figure 19. Scheme of the Eu(III)-IIM/PC/SPE structure

A Differential Pulse Adsorptive Stripping Voltammetry (DPASV) approach was employed and the peak-current intensity was used as output signal. The analytical conditions were optimized, finding that the best performance is obtained using acetate buffer at pH =4.7 with accumulation potential and time measure of -0.2 V and 300 s, respectively. In these conditions, the DPASV response to Eu(III), as peak-current intensity, increases along with Eu(III) concentration, with a detection limit of $1.0 \cdot 10^{-7}$ mol dm^{-3} . The presence of other metal ions such as Na(I), Ca(II), Mg(II), Zn(II), Ni(II), Fe(II), Co(II) and Cu(II), at concentration levels 500 times higher than those of Eu(III) as well as Ho(III), Dy(III), Er(III), Ce(III), Gd(III), Pr(III), Nd(III), Tb(III) and Yb(III) 50 times more concentrated than Eu(III), caused a variation of the peak current within $\pm 5\%$, indicating the high selectivity of the system towards Eu(III) ions detection. The results

reported suggest that the Eu(III)-IIM/PC/SPE system shows high sensitivity and stability to be used as electrochemical sensor to determine Eu(III) ion also in complex matrices such as environmental water samples.

H. A. Zamani *et al.* developed some Gd(III) selective polyvinylchloride (PVC) membrane sensors using different molecules as selectophores [63-66]. As an example, the sensor containing N'-(2-oxo-1,2-di(pyridin-2-yl)ethylidene)furan-2-carbohydrazide (**L19**) (Scheme 11) as ionophore [62] is reported. This system is based on a bulb-shaped PVC membrane that separates an internal standard solution containing a known concentration of GdCl₃ and the external solution to be analyzed. The PVC membrane contains a ionophore to make it able to conduct electricity and a ligand suitable to reversibly coordinating Gd(III). When the membrane separates two solutions with different concentration of Gd(III), an electric potential difference between the two sides forms due to the different amount of ions linked to the two surfaces (Figure 20); when this potential difference is proportional to the concentration of Gd(III) in the analytical solution the membrane shows a "nernstian behaviour".

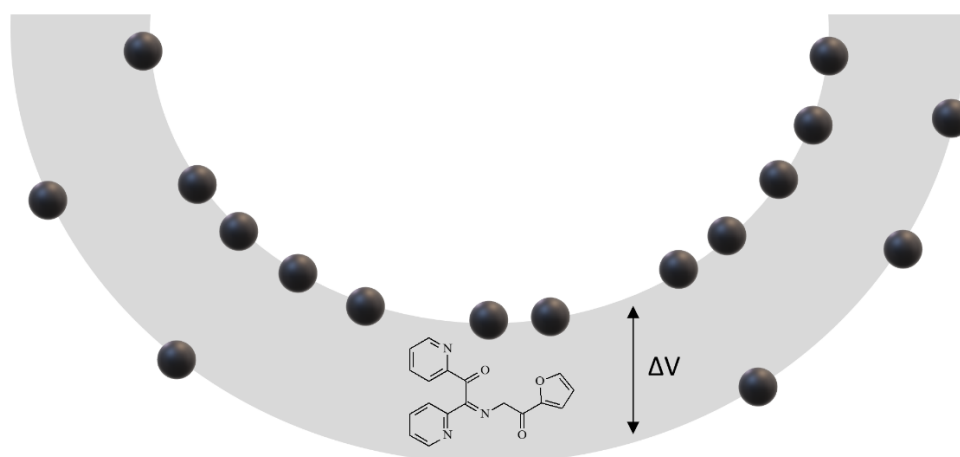
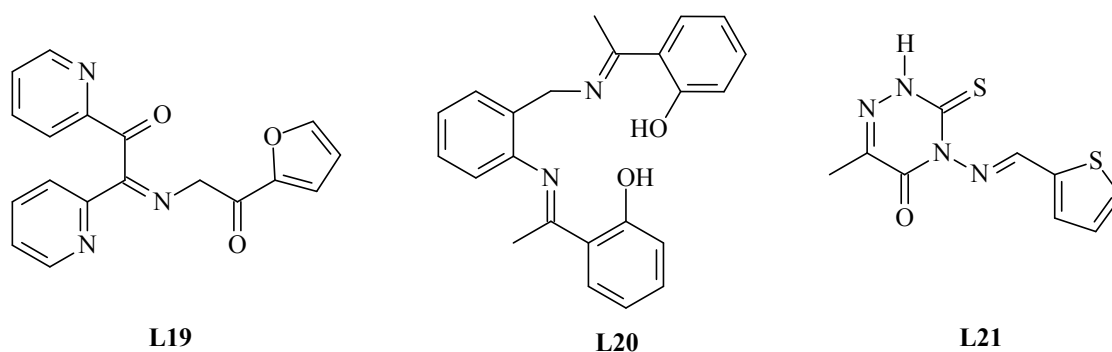


Figure 20. Representation of the electrical potential established due to the concentration difference of GdCl₃ solution between the sides of the bulb-shaped PVC membrane.

The membrane potential can be measured using two reference electrodes, for example an internal silver electrode and an external saturate calomel electrode (SCE), building a galvanic cell with this scheme: Ag–AgCl | $1.0 \cdot 10^{-3} \text{ mol} \cdot \text{dm}^{-3} \text{ GdCl}_3$ | PVC membrane: test solution | Hg–Hg₂Cl₂, KCl (satd).

The molecules used as selectophores to make the membranes sensitive to Gd(III) ions are mainly represented by a series of ligands based on Schiff-base or hydrazone groups able to selectively bind Gd(III), some examples are reported in Scheme 11.



Scheme 11. Structures of the molecules used as selectophores

8. CONCLUSION AND OUTLOOKS

Nowdays the coordination and supramolecular chemistry of trivalent rare earth ions are seeing an impressive rising in interest due to the ever-growing need of luminescent chemosensors for medical diagnostic and new contrast agents to use in magnetic resonance imaging. At the same time, the use of rare earth elements for modern applications are countless, ranging from components of common technological devices to innovative functional materials. Due to their wide diffusion, many researchers have

been stimulated to develop sensors with the aim to detect rare earth metal ions. In the field of sensor design, the main crucial parameters are the sensitivity and selectivity towards the detected target; a chemosensor often possesses both parameters, being a molecular system responding to the presence of the target by an easy-to-monitor response that can be an optical, fluorescent or electrochemical output. In the case of rare earth metal ions, the design of selective chemosensors is a hard challenge mainly because of their poor coordination properties in aqueous environment. In fact, even though there are a lot of Ln(III) complexes used as functional materials and contrast agents, only few examples of ligands acting as efficient chemosensors for these metal ions were described. For this reason, researchers tried to exploit not only classic fluorescence ligands containing a receptor and a fluorophore linked through a spacer, but also more complexed systems, like supramolecular aggregates based on micelles, graphene sheets, Quantum Dots and Carbon Dots or bio-engineered paradigms. In the last case, natural or semi-synthetic proteins able to selectively and strongly bind Ln(III) ions over other common metal ions were employed. In conclusion, at the moment this research field offers a lot of intriguing possibilities and, as above mentioned, multidisciplinarity is absolutely necessary, involving organic and inorganic chemists, electrochemists, physical-chemists, physicists, biochemists and material engineers.

ACKNOWLEDGMENTS

The authors thank:

Italian Ministero dell'Istruzione dell'Università e della Ricerca, (MIUR) (project

2017EKCS35).

University of Urbino (Department of Pure and Applied Sciences – Grant DISPEA_GIORGI_PROG20, DISPEA_MATTIOLI_PROG20).

REFERENCES

- [1] P. Ebrahimi; M. Barbieri, Gadolinium as an Emerging Microcontaminant in Water Resources: Threats and Opportunity, *Geosciences* 9 (2019) 93-137.
<https://doi.org/10.3390/geosciences9020093>.
- [2] P. Möller, M. Bau, P. Dulski, V. Lüders, REE and yttrium fractionation in fluorite and their bearing on fluorite formation, *Proceedings of the Ninth Quadrennial IAGOD Symposium*, E. Schweizerbart'sche Verlagsbuchhandlung, Stuttgart, Germany, 1998.
- [3] H. Öztürk, S. Altuncu, N. Haniççi, C. Kasapçı, K. M. Goodenoughc, Rare earth element-bearing fluorite deposits of Turkey: An overview, *Ore Geology Reviews* 105 (2019) 423-444.
- [4] N. N. Greenwood, A. Earnshaw, *Chemistry of the Elements*, third edition, Elsevier Limited, Oxford, UK, 2016.
- [5] Separation of Promethium From a Natural Lanthanide Mixture. By: Erametsa, O, *Acta Polytechnica Scandinavica-Chemistry Including Metallurgy Series*, Issue: 37 Pages: 1-&, Published: 1965.
- [6] Default Soil Solid Liquid Partition-Coefficients, Kds, For 4 Major Soil Types - A Compendium, By: Sheppard, Mi; Thibault, Dh; *Health Physics*, Volume: 59, Issue: 4, Pages: 471-482, Published: OCT 1990.

- [7] A. Kabata-Pendias, A.B. Mukherjee, Trace Elements from Soil to Human, Springer Berlin Heidelberg, 2007.
- [8] J. Gaillardet, J. Viers, B. Dupré, Trace Elements in river waters, *Treatise on Geochemistry* 5 (2003) 225-272. <https://doi.org/10.1016/B0-08-043751-6/05165-3>.
- [9] K. H. Wedepohl, The composition of the continental crust, *Geochimica et Cosmochimica Acta* 59 (1995) 1217-1232. [https://doi.org/10.1016/0016-7037\(95\)00038-2](https://doi.org/10.1016/0016-7037(95)00038-2).
- [10] D. Schüler, M. Buchert, R. Liu, S. Degreif, C. Merz, Study on Rare Earths and Their Recycling, OKO-insitut e.V., Germany, Darmstadt, 2011.
- [11] Engineering Technical Support Center Land Remediation and Pollution Control Division National Risk Management Research Laboratory Office of Research and Development Cincinnati, Rare Earth Elements: A Review of Production, Processing, Recycling, and Associated Environmental Issue, National Service Center for Environmental Publications (NSCEP), EPA, 2012.
- [12] J.-C. G. Bünzli, Benefiting from the Unique Properties of Lanthanide Ions, *Acc. Chem. Res.* 39 (2006) 53-61. <https://doi.org/10.1021/ar0400894>.
- [13] a) C. M.G. dos Santos, A. J. Harte, S. J. Quinn, T. Gunnlaugsson, Recent developments in the field of supramolecular lanthanide luminescent sensors and self-assemblies, *Coord. Chem. Rev.* 252 (2008) 2512-2527. <https://doi.org/10.1016/j.ccr.2008.07.018>. b) D. E. Barry, D. F. Caffrey, T. Gunnlaugsson, Lanthanide-directed synthesis of luminescent self-assembly supramolecular structures and mechanically bonded systems from acyclic coordinating organic ligands, *Chem. Soc. Rev.* 45 (2016) 3244-3274. <https://doi.org/10.1039/C6CS00116E>.
- [14] J.-C. G. Bünzli, D. Wessner, Complexes of the Lighter Lanthanoid Nitrates with 15-crown-5 and 18-crown-6 ethers: Synthesis and characterization, *Helvetica Chimica Acta*, 61 (1978) 1454-1461. <https://doi.org/10.1002/hlca.19780610429>.

- [15] J.-C. G. Bünzli, D. Wessner, B. Klein, Complexes of the Heavier Lanthanoid Nitrates with Crown Ethers. In: McCarthy G.J., Rhyne J.J., Silber H.B. (eds) *The Rare Earths in Modern Science and Technology*. Springer, Boston, MA. 2016. https://doi.org/10.1007/978-1-4613-3054-7_18.
- [16] S. T. Mullins, P. G. Sammes, R. M. West, G. Yahioğlu, Preparation of Some New Intercalating Europium(III) Sensitizers, *Journal of the Chemical Society-Perkin Transactions 1* (1996) 75-81. <https://doi.org/10.1039/P19960000075>.
- [17] C. Benelli, E. Borgogelli, M. Formica, V. Fusi, L. Giorgi, E. Macedi, M. Micheloni, P. Paoli, P. Rossi, Di-maltol-polyamineligands to form heterotrinnuclear metal complexes: solid state, aqueous solution and magnetic characterization, *Dalton Trans.* 42 (2013) 5848-5859. <https://doi.org/10.1039/C3DT32130D>.
- [18] S. Amatori, G. Ambrosi, M. Fanelli, M. Formica, V. Fusi, L. Giorgi, E. Macedi, M. Micheloni, P. Paoli, P. Rossi, A Preorganized Metalloreceptor for Alkaline Earth Ions Showing Calcium Versus Magnesium Selectivity in Water: Biological Activity of Selected Metal Complexes, *Chemistry - A European Journal* 20 (2014) 11048-11057. <https://doi.org/10.1002/chem.201403084>.
- [19] P. Rossi, S. Ciattini, M. Formica, V. Fusi, L. Giorgi, E. Macedi, M. Micheloni, P. Paoli, 3d-4f-3d trinuclear complexes with di-maltol-polyamine ligands. Solid state structure and solution behaviour, *Inorg. Chim. Acta* 470 (2018) 254-262. <https://doi.org/10.1016/j.ica.2017.06.033>.
- [20] A. Bremer, A. Geist, P. J. Panak, Complexation of Cm(III) with 6-(5,6-dipentyl-1,2,4-triazin-3-yl)-2,2'-bipyridine studied by time resolved laser fluorescence spectroscopy, *Dalton Trans.* 41 (2012) 7582-7589. <https://doi.org/10.1039/C2DT30541K>.
- [21] C. Wagner, U. Müllich, A. Geist, P. J. Panak, TRLFS study on the complexation of Cm(III) and Eu(III) with SO₃-Ph-BTBP, *Dalton Trans.* 44 (2015) 17143-17151. <https://doi.org/10.1039/c5dt02923f>.

- [22] R. Akbar, M. Baral, B.K. Kanungo, The influence of europium(III) and terbium(III) on the electronic system of impudent tripodal ligand: Binding, spectrophotometric and theoretical investigations, *J. Photochem. Photobiol. A: Chemistry* 287 (2014) 49-64. <https://doi.org/10.1016/j.jphotochem.2014.04.019>.
- [23] R. Akbar, M. Baral, B.K. Kanungo, Experimental and theoretical approach of photophysical properties of lanthanum(III) and erbium(III) complexes of tris(methoxymethyl)-5-oxine podant, *Spectrochimica Acta Part A: Molecular and Biomolecular Spectroscopy* 129 (2014) 365-376. <https://doi.org/10.1016/j.saa.2014.03.045>.
- [24] K. Guzow, M. Milewska, D. Wróblewski, A. Gieldon, W. Wiczak, 3-[2-(8-Quinoliny)benzoxazol-5-yl]alanine derivative—a specific fluorophore for transition and rare-earth metal ion detection, *Tetrahedron* 60 (2004) 11889-11894. <https://doi.org/10.1016/j.tet.2004.09.084>.
- [25] B.S. Lukyanov, M.B. Lukyanova, Spiropyrans: Synthesis, Properties and Application. (Review), *Chem. Heterocyc. Compd.* 41 (2005) 281-311. <https://doi.org/10.1007/s10593-005-0148-x>.
- [26] K. Kruttwig, D.R. Yankelevich, C. Brueggemann, C. Tu, N. L'Etoile, A. Knoesen, A.Y. Louie, Reversible Low-Light Induced Photoswitching of Crowned Spiropyran-DO3A Complexed with Gadolinium(III) ions. *Molecules* 17 (2012) 6605-6624. <https://doi.org/10.3390/molecules17066605>.
- [27] Z. Liu, L. Jiang, Z. Liang, Y. Gao, A selective colorimetric chemosensor for lanthanide ions, *Tetrahedron* 62 (2006) 3214-3220. <https://doi.org/10.1016/j.tet.2006.01.073>.
- [28] O.G. Nikolaeva, O. Yu Karlutova, A.S. Cheprasov, K.S. Tikhomirova, Y.V. Revinskii, E.N. Shepelenko, Zh.V. Bren, O.G. Karamov, A.V. Metelitsa, A.D. Dubonosov, V.A. Bren, V.I. Minkin, Photo- and Ionochromic Spiroindoline-2,2'-pyrano[2,3-f]chromenecarbohydrazides- Chemosensor for Lanthanide Cations, *Doklady Chemistry* 480 (2018) 121-125. <https://doi.org/10.1134/S0012500818060071>.

- [29] Y. Guo, F. Huo, C. Yin, J. Kang, J.F. Li, A highly selective and sensitive turn-on fluorescent probe for the detection of holmium ion and its bioimaging, *RSC Adv.* 5 (2015) 10845-10848. <https://doi.org/10.1039/C4RA15530K>.
- [30] M. Formica, V. Fusi, L. Giorgi, M. Micheloni, New fluorescent chemosensors for metal ions in solution, *Coordination Chemistry Reviews* 256 (2012) 170-192. <https://doi.org/10.1016/j.ccr.2011.09.010>.
- [31] S. Sasaki, G.P.C. Drummen, G. Konishi, Recent advances in Twisted Intramolecular Charge Transfer (TICT) fluorescence and related phenomena in materials chemistry, *J. Mater. Chem. C* 4 (2016) 2731-2743. <https://doi.org/10.1039/C5TC03933A>.
- [32] F. Faridbod, M. Sedaghat, M. Hosseini, M. R. Ganjali, M. Khoobi, A. Shafiee, P. Norouzi, Turn-on fluorescent chemosensor for determination of lutetium ion, *Spectrochimica Acta Part A: Molecular and Biomolecular Spectroscopy* 137 (2015) 1231-1234. <https://doi.org/10.1016/j.saa.2014.08.024>.
- [33] Z. Liang, Z. Liu, Y. Gao, A selective colorimetric chemosensor based on calixarene framework for lanthanide ions-Dy³⁺ and Er³⁺, *Tetrahedron Letters* 48 (2007) 3587-3590. <https://doi.org/10.1016/j.tetlet.2007.03.086>.
- [34] I.E. Tolpygin, K.S. Tikhomirova, Y.V. Revinskii, Z.V. Bren, A.D. Dubonosov, V.A. Bren, *o*-Nitroarylidene imines, bifunctional fluorescent chemosensors for lanthanide cations and fluoride anions, *Russian Journal of Organic Chemistry* 53 (2017) 1651-1654. <https://doi.org/10.1134/S1070428017110057>.
- [35] M. Liu, Z. Xu, Y. Song, H. Li, C. Xian, A novel coumarin-based chemosensor for colorimetric detection of Ag(I) ion and fluorogenic sensing of Ce(III) ion, *Journal of Luminescence* 198 (2018) 337-341. <https://doi.org/10.1016/j.jlumin.2018.02.047>.
- [36] T. Yu, J. Meng, Y. Zhao, H. Zhang, X. Han, D. Fan, Synthesis and rare earth metal ion-sensing properties of aza-crown derivative incorporating with diaryl-1,3,4-oxadiazole, *Spectrochimica Acta Part A: Molecular and Biomolecular Spectroscopy* 78 (2011) 396-400. <https://doi.org/10.1016/j.saa.2010.10.027>.

- [37] R.S. Kumar, S.K.A. Kumar, K. Vijayakrishna, A. Sivaramakrishna, C.V.S. B. Rao, N. Sivaraman, S.K. Sahoo, Highly selective CHEF-type chemosensor for lutetium (III) recognition in semi-aqueous media, *Spectrochimica Acta Part A: Molecular and Biomolecular Spectroscopy* 214 (2019) 32-39.
<https://doi.org/10.1016/j.saa.2019.02.003>.
- [38] W.S. Xia, R.H. Schmehl, C.J. Li, A Fluorescent 18-Crown-6 Based Luminescence Sensor for Lanthanide Ions, *Tetrahedron* 56 (2000) 7045-7049.
[https://doi.org/10.1016/S0040-4020\(00\)00528-7](https://doi.org/10.1016/S0040-4020(00)00528-7).
- [39] H. Liang, X. Deng, M. Bosscher, Q. Ji, M.P. Jensen, C. He, Engineering Bacterial Two-Component System PmrA/PmrB to Sense Lanthanide Ions, *J. Am. Chem. Soc.* 135 (2013) 2037-2039. <https://doi.org/10.1021/ja312032c>.
- [40] K.J Franz, M. Nitz, B. Imperiali, Lanthanide-Binding Tags as Versatile Protein Coexpression Probes, *ChemBioChem* 4 (2003) 256-271.
<https://doi.org/10.1002/cbic.200390046>.
- [41] J.A. Mattocks, J.V. Ho, J.A. Cotruvo Jr, A Selective, Protein-Based Fluorescent Sensor with Picomolar Affinity for Rare Earth Elements, *J. Am. Chem. Soc.* 141 (2019) 2857-2861. <https://doi.org/10.1021/jacs.8b12155>.
- [42] E.C. Cook, E.R. Featherston, S.A. Showalter, J.A. Cotruvo Jr., Structural Basis for Rare Earth Element Recognition by *Methylobacterium extorquens* Lanmodulin, *Biochemistry* 58 (2019) 120-125. <https://doi.org/10.1021/acs.biochem.8b01019>.
- [43] J.A. Cotruvo Jr., E.R. Featherston, J.A. Mattocks, J.V. Ho, T.N. Laremore, Lanmodulin: a Highly Selective Lanthanide-Binding Protein from a Lanthanide-Utilizing Bacterium, *J. Am. Chem. Soc.* 140 (2018) 15056-15061.
<https://doi.org/10.1021/jacs.8b09842>.
- [44] A.E. Palmer, M. Giacomello, T. Kortemme, S.A. Hires, V. Lev Ram, D. Baker, R.Y. Tsien, Ca²⁺ Indicators Based on Computationally Redesigned Calmodulin-Peptide Pairs, *Chem. Biol.* 13 (2006) 521-530. <https://doi.org/10.1016/j.chembiol.2006.03.007>.

- [45] S. Wang, L. Ding, J. Fan, Z. Wang, Y. Fang, Bispyrene/Surfactant-Assembly-Based Fluorescent Sensor Array for Discriminating Lanthanide Ions in Aqueous Solution, *ACS Appl. Mater. Interfaces* 6 (2014) 16156-16165.
<https://doi.org/10.1021/am504208a>.
- [46] J. Lu, I. Do, L.T. Drzal, R.M. Worden, I. Lee, Nanometal-Decorated Exfoliated Graphite Nanoplatelet Based Glucose Biosensors with High Sensitivity and Fast Response, *ACS Nano* 2 (2008) 1825-1832. <https://doi.org/10.1021/nn800244k>.
- [47] S. Zhu, S. Tang, J. Zhang, B. Yang, Control the size and surface chemistry of graphene for the rising fluorescent materials, *Chem. Commun.* 48 (2012) 4527-4539.
<https://doi.org/10.1039/C2CC31201H>.
- [48] F. Salehnia, F. Faridbod, A.S. Dezfuli, M.R. Ganjali, P. Norouzi, Cerium(III) Ion Sensing Based on Graphene Quantum Dots Fluorescent Turn-Off, *J. Fluoresc.* 27 (2017) 331-338. <https://doi.org/10.1007/s10895-016-1962-5>.
- [49] D.J. Dmonte, A. Pandiyarajan, N. Bhuvanesh, S. Suresh, R. Nandakumar, Graphene oxide resorcinol hybrid material as fluorescent chemosensor for detection of cerium ion, *Materials Letters* 227 (2018) 154-157.
<https://doi.org/10.1016/j.matlet.2018.05.051>.
- [50] D. Bera, L. Qian, T.-K. Tseng, P.H. Holloway, Quantum Dots and Their Multimodal Applications: A Review, *Materials* 3 (2010) 2260-2345.
<https://doi.org/10.3390/ma3042260>.
- [51] R.E. Galian, M. Guardia, The use of quantum dots in organic chemistry, *Trends Anal. Chem.* 28 (2009) 279-291. <https://doi.org/10.1016/j.trac.2008.12.001>.
- [52] R. Freeman, I. Willner, Optical molecular sensing with semiconductor quantum dots (QDs), *Chem. Soc. Rev.* 41 (2012) 4067-4085.
<https://doi.org/10.1039/C2CS15357B>.
- [53] M.K. Rofouei, N. Tajarrood, M. Masteri-Farahani, R. Zadmard, A New Fluorescence Sensor for Cerium (III) Ion Using Glycine Dithiocarbamate Capped

Manganese Doped ZnS Quantum Dots, *J. Fluoresc.* 25 (2015) 1855-1866.

<https://doi.org/10.1007/s10895-015-1678-y>.

[54] X. Chu, S. Wang, Y. Cao, A new fluorescence probe comprising nitrogen-doped graphene quantum dots for the selective and quantitative determination of cerium(IV), *New J. Chem.* 44 (2020) 797-806. <https://doi.org/10.1039/C9NJ04518J>.

[55] M.L. Liu, B.B. Chen, C.M. Li, C.Z. Huang, Carbon dots: synthesis, formation mechanism, fluorescence origin and sensing applications, *Green Chem.* 21 (2019) 449-471. <https://doi.org/10.1039/C8GC02736F>.

[56] S. Anwar, H. Ding, M. Xu, X. Hu, Z. Li, J. Wang, L. Liu, L. Jiang, D. Wang, C. Dong, M. Yan, Q. Wang, H. Bi*, Recent Advances in Synthesis, Optical Properties, and Biomedical Applications of Carbon Dots, *ACS Appl. Bio Mater.* 2 (2019) 2317-2338. <https://doi.org/10.1021/acsabm.9b00112>.

[57] S. Dolay, S. K. Bhunia, L. Zeiri, O. Paz-Tal, R. Jelinek, Thenoyltrifluoroacetone (TTA)-Carbon Dot/Aerogel Fluorescent Sensor for Lanthanide and Actinide Ions, *ACS Omega* 2 (2017) 9288-9295. <https://doi.org/10.1021/acsomega.7b01883>.

[58] M.R. Ganjali, M. Hosseini, M. Khobi, S. Farahani, M. Shaban, F. Faridbod, A. Shafiee, P. Norouzi, A novel europium-sensitive fluorescent nano-chemosensor based on new functionalized magnetic core-shell Fe₃O₄@SiO₂ nanoparticles, *Talanta* 115 (2013) 271-276. <https://doi.org/10.1016/j.talanta.2013.04.010>.

[59] C.M.A. Brett, Electrochemical sensors for environmental monitoring. Strategy and examples, *Pure Appl. Chem.* 73 (2001) 1969-1977. <https://doi.org/10.1351/pac200173121969>.

[60] X.Z. Li, Y.P. Sun, Evaluation of ionic imprinted polymers by electrochemical recognition of rare earth ions, *Hydrometallurgy* 87 (2007) 63-71. <https://doi.org/10.1016/j.hydromet.2007.02.003>.

- [61] G.D. Brindley, O.D. Fox, P.D. Beer, Ferrocene-appended and bridged calixareneligands for the electrochemical sensing of trivalent lanthanide ions, *Dalton Trans.* (2000) 4354-4359. <https://doi.org/10.1039/B007146N>.
- [62] J. Chen, H. Bai, J. Xia, Z. Li, P. Liu, Q. Cao, Electrochemical sensor for detection of europium based on poly-catechol and ion-imprinted sol-gel film modified screen-printed electrode, *J. Electroanal. Chem.* 824 (2018) 32-38. <https://doi.org/10.1016/j.jelechem.2018.07.015>.
- [63] H. A. Zamani, G. Rajabzadeh, M. R. Ganjali, P. Norouzi, Determination of gadolinium(III) ions in soil and sediment samples by a novel gadolinium membrane sensor based on 6-methyl-4- {[1-(2-thienyl)methylidene]amino} 3-thioxo-3,4-dihydro-1,2,4-triazin-5-(2H)-one, *Analytica Chimica Acta* 598 (2007) 51-57. <https://doi.org/10.1016/j.aca.2007.07.028>.
- [64] H. A. Zamani, M. Mohammadhosseini, S. H. Mohammadrezazadeh, F. Faridbod, M. R. Ganjali, S. Meghdadi, A. Davoodnia, Gadolinium(III) ion selective sensor using a new synthesized Schiff's base as a sensing material, *Materials Science and Engineering: C* 32 (2012) 712-717. <https://doi.org/10.1016/j.msec.2012.01.013>.
- [65] H. A. Zamani, H. Behmadi, Gadolinium(III) Ion-Selective Electrode Based on 3-Methyl-1H-1,2,4-triazole-5-thiol, *E-Journal of Chemistry* 9 (2012) 308-312. <https://doi.org/10.1155/2012/239245>.
- [66] H. A. Zamani, F. Faridbod, M. R. Ganjali, A new selectophore for gadolinium selective sensor, *Materials Science and Engineering: C*, 43 (2014) 488-493. <https://doi.org/10.1016/j.msec.2014.07.035>.